ESA STR-223
September 1987

A laboratory study of tin whisker growth

B.D. Dunn
European Space Research and Technology Centre
Noordwijk, The Netherlands

european space agency
agence spatiale européenne

ESA STR-223
September 1987

A laboratory study of tin whisker growth

B.D. Dunn
European Space Research and Technology Centre
Noordwijk, The Netherlands

european space agency / agence spatiale européenne
8-10, rue Mario-Nikis, 75738 PARIS CEDEX 15, France

Approved for publication by M.C. Le Fèvre, Director of ESTEC

Report published and distributed by ESA Publications Division
ESTEC, Noordwijk, The Netherlands

Edited by W.R. Burke & B. Battrick

Printed in The Netherlands

Price code E1

International Standard Serial Number ISSN 0379 4067

ABSTRACT

This work is devoted to a metallurgical analysis of the mechanism of spontaneous tin whisker growths.

Laboratory investigations relate the ubiquity of whiskers to particular types of tin plating and characteristics of the substrate material. New whisker morphologies have been discovered and they may have diameters of only 6 nm, although the majority are in the order of 4 μm diameter with lengths approaching 2 mm. A major finding was that compressive stresses applied to the tin plate did not accelerate whisker growth rates. Nodular eruptions are frequently observed to precede those whiskers with short incubation times.

Crystallography has identified five whisker growth directions. Together with TEM studies, they are shown to be single crystals containing no dislocations or second phases. White to grey tin allotropic transformation at cryogenic temperatures could not be induced.

A concise five-stage model to account for the spontaneous growth of tin whiskers is proposed, based on the results of the detailed test programme. It is strongly recommended that surfaces known to nucleate whisker growths be excluded from the designs of high-reliability equipment. Methods for the prevention of whiskers are put forward, together with a selection of alternative finishes found to be immune to such growth phenomena.

CONTENTS

ACKNOWLEDGEMENTS

The author is grateful to the European Space Agency which provided some support for this study and is indebted to Mr. D.E.J. Talbot and the late Mr. B.L. Davies for useful discussions during the writing of this report.

He also thanks Dr. J.W. Visser of the Dutch Institute for Physics for assistance with the X-ray diffraction oscillation camera. Invaluable technical assistance was offered by Messrs. H. Mandriej (Twente University) and N. Droste (Dutch Metal Institute) in connection with, respectively, the 200 keV and 1 MeV transmission electron-microscope facilities.

A LABORATORY STUDY OF TIN WHISKER GROWTH

1. INTRODUCTION

Whiskers are fibrous growths of solid substances, either metallic or non-metallic. They have length-to-diameter ratios that are frequently greater than 1000 and uniform cross-sections having a high degree of internal and external perfection. Though their appearance and mechanism of growth may be captivating, unwanted growths can cause catastrophic failures. Exasperating electrical short-circuits are known to have been produced in low-voltage equipment by whiskers that remain conducting (up to around 30 mA) between two circuit lines. They can also create debris and contaminate the smooth running of micromechanical systems.

Past investigations into tin whisker growth mechanisms have arrived at different and, to some extent, contradictary results. This may be because the specimens were not prepared in the same way, resulting in the recording of some different fundamental effects. For instance, Arnold [1] reports that virtually no tin whiskers form on tin-plated brass, whereas Britton [2] has shown this to be a substrate providing prolific whisker growths. Probably one of works most frequently referred to, that of Fisher and co-workers [3], describes how the growth rate of tin whiskers can be accelerated up to 10 000 times the observed spontaneous rate by the application of pressure. However, the bent samples of tin-plated sheets depicted in several of the early papers do not indicate any preferential growth locations, or rates of growth, on areas that might be under severe mechanical compressive stress.

The present study was undertaken to reveal more information about the phenomenon of whisker growth. One objective of this laboratory work was to select methods likely to obviate the occurrence of such growths. The test method involved the plating of various forms of tin onto C-rings machined and prepared with different material finishes. The sample permutations were selected both to re-examine the conditions known to induce whisker growth and to introduce new factors thought likely to promote growth. The main variables consisted of:

- two different substrate materials
- three forms of tin-plate
- half of the total number of specimens supported a copper-plated barrier layer between substrate and tin finish
- certain tin finishes were melted (fused)
- three stress levels were applied to the specimens.

In order to avoid the introduction of unintentional minor variations, the whisker-growth specimens were fabricated to very close tolerances (overall dimensions and plating thicknesses), manufactured in the same time period (some two days) and plated under identical conditions (under full quality-assurance surveillance). Close attention was paid to the calculation of the stress levels and their application to the specimens.

2. EXPERIMENTAL PROCEDURES

2.1 DESCRIPTION OF TEST SPECIMEN

The samples consisted essentially of machined C-rings, rather similar to those designed for stress corrosion testing. The specimens could be stressed by constant deflection using a nut and bolt which were tightened until the sides were pulled together to give the desired stress. The bolts were inserted in diametrically opposite holes drilled through each ring wall. The materials selected and the dimensions of the C-ring test specimens are identified in Figure 1.

The choice of the C-ring specimen design allowed whisker growths to be observed on the compressively stressed inner wall, on the tensile stressed outer wall, and at local points around the nut, washer and bolt, which would be held under high compressive loads.

Two substrate materials were chosen for the experiment:

— 60−40 brass, seen by some experimenters to promote whisker growth
— plain carbon steel, seen by some experimenters to be a substrate immune to whisker growth.

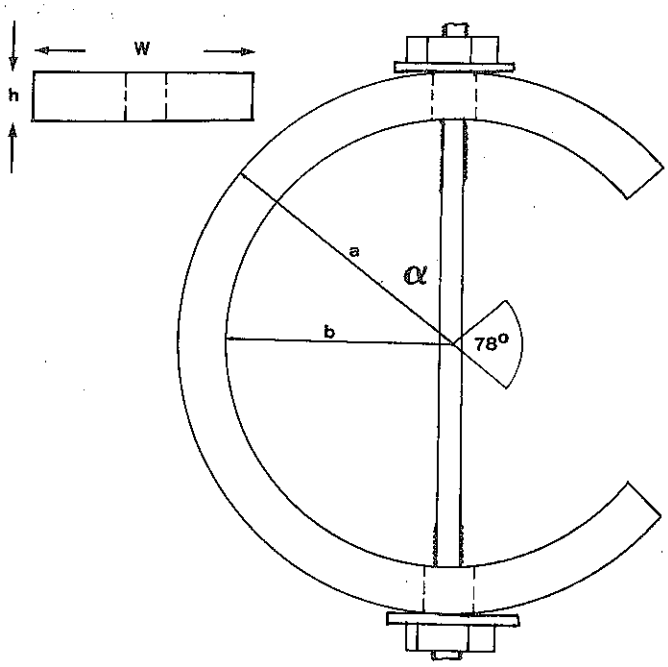

DIMENSIONS:

W = width = 10 cm
h = thickness = 2 mm
a = outside radius = 12.5 mm
b = inside radius = 10.5 mm
all tolerances ±0.02 mm
Threads: all size M2
Very high quality machine-finish

MATERIALS:

C-rings 60−40 brass 1/2 hard
or
0.2 carbon steel
Bolts 0.2 carbon steel
Nuts 304 stainless steel
Washer 304 stainless steel

Figure 1. Overall dimensions and identification of materials for C-ring specimens

2.2 PLATING PROCEDURES

2.2.1 Tin-plating conditions

Previous work has indicated that the causes of whisker growth are related to conditions of the plating bath. The plating bath employed for this study was based on a tin sulphate electrolyte and was a standard commercial process. Acid-resistant, plastic-lined steel-plating tanks were employed, with suitable filtration equipment to remove any solid particles or precipitated matter from the solution. This would curtail porosity and roughness of the tin deposit. The tin anodes and tin salts for electroplating conformed to national-specification purity levels. The tin anode contained a minimum of 99.75% tin, with maximum limits of 0.08% antimony, 0.08% lead and 0.05% copper. The anodes were bagged with an acid-resisting Dacron-type material to prevent solution contamination by any detached particles which might have caused deposit roughness.

Full details of the plating currents and the analytical results for each type of plating are listed in Table 1. The electrolyte analyses were confirmed by test-laboratory analyses made on samples extracted from the baths.

The C-rings were plated with 5 μm thickness of tin, under the following conditions:

- normal tin (as used commercially)
- abnormal tin (with high current density to provide deposit with compressive stress)
- organically contaminated tin (flour dust was used to plate-in occlusions). Filtration was not applied to this bath.

2.2.2 Copper intermediate layer

Half of the total number of specimens were plated with an intermediate barrier layer of 3 μm thick copper between the C-ring substrate and the final tin-plating. This pure copper was plated from a copper cyanide bath at 1.5 A/dm^2 (temperature 20°C, pH 9.7 to procedure H-307).

TABLE 1. *Bath conditions for the various tin platings*

	NORMAL TIN	ABNORMAL TIN	ORGANICALLY CONTAMINATED TIN
Tin as stannous sulphate (g/l)	40	7.5	40
Free sulphuric acid (g/l)	160	160	160
Oxymetal brightener no. 4 (cc/l)	10	10	10
no. 5 (cc/l)	4	4	4
no. 6 (cc/l)	20	20	20
Organic flour contamination	none	none	handful
Bath temperature	20°C	50°C	30°C
Current density (agitated bath)	1.5 A/dm^2	5 A/dm^2	1.5 A/dm^2

NOTE: All chemical analyses confirmed by analysis reports from Oxymetals Benelux Laboratories.

Table 2 identifies the various C-ring samples and lists the nominal copper- and tin-plating thicknesses.

2.3 REFLOWING (FUSING) OF TIN-PLATE

The fusing of tin-lead electroplatings onto the copper conductors of printed-circuit boards by asymptotic heating in high-temperature oils has proved to be a suitable and controllable process [4] for eutectic alloys that melt at approximately 183°C. The higher melting point of tin, at 232°C, caused degradation of the usual fusing oils and constituted a fire risk so, instead, certain of the 'normal' tin-plated C-ring specimens were subjected to fusion in a fluidised sand-bath furnace. The furnace was held at 250°C under a flow of nitrogen to prevent oxidation of the tin-plate. Each C-ring was immersed in the fluidised sand for 25 s in order to achieve a flat, reflowed tin finish.

2.4 APPLICATION OF STRESS TO C-RINGS

Forty C-rings were subjected to the whisker-growth experiment. Each combination of substrate material and plating finish was tested in triplicate (with the exception of the fused-tin samples), each specimen being tested under 'zero', 'slight', or 'high' applied loads. The full specimen identifications are listed in Table 2.

Photographs of the C-ring samples are shown in Figure 2.

The C-rings were loaded by tightening the nuts on the bolt; this produced deflection of the C-ring so that the inner surface became compressed. Compressive test stresses applied to the various tin platings were:

'slight' stress = 5 kg/mm^2
'high' stress = 40 kg/mm^2

Calculations of the deflections required to cause these compressive stresses have been made on the basis of data provided in References 5 and 6.

Note that the maximum test stresses are applied at 90° to the C-ring axis, so that sin $\alpha = 1$. There will be a progressive reduction in resultant stress along each quadrant as the factor sin α tends to zero.

2.5 EXAMINATION OF GROWTHS

2.5.1 Storage conditions

The plated C-ring specimens were inspected for surface irregularities within 24 h of the final electroplating process. The samples were then stored within a large compartmentalised perspex housing, enclosed inside a polythene package. Samples were only handled with tweezers applied to the threaded portion of the central bolt (Fig. 2). The storage environment was that of a laboratory maintained within the temperature range 15−23°C at an estimated relative humidity of 40−80%. Unplated controls were also stored. To date, they show no evidence of tarnish or oxidation.

TABLE 2. *Identification of C-ring specimens and plating thickness data*

SPECIMEN	BASE	PLATING LAYER(s) (nominal thickness) (μm)	APPLIED STRESS-LEVEL	ACTUAL PLATING THICKNESS FROM MICRO-SECTIONS* (μm)
1	Brass	5 normal Sn	none	8
2			slight	
3			high	
4		5 abnormal Sn	none	5
5			slight	
6			high	
7		5 organic contaminated	none	8
8			slight	
9			high	
10		3 Cu + 5 normal Sn	none	1.5 + 6
11			slight	
12			high	
13		3 Cu + 5 abnormal Sn	none	1.5 + 3
14			slight	
15			high	
16		3 Cu + 5 organic cont.	none	1.5 + 8
17			slight	
18			high	
19		5 normal Sn fused	high	8
20		3 Cu + 5 normal Sn fused	high	1.5 + 8
21	Steel	5 normal Sn	none	8
22			slight	
23			high	
24		5 abnormal Sn	none	4
25			slight	
26			high	
27		5 organic contaminated	none	5
28			slight	
29			high	
30		3 Cu + 5 normal Sn	none	2 + 8
31			slight	
32			high	
33		3 Cu + 5 abnormal Sn	none	2 + 5
34			slight	
35			high	
36		3 Cu + 5 organic cont.	none	2 + 6
37			slight	
38			high	
39		5 normal Sn fused	high	8
40		3 Cu + 5 normal Sn fused	high	1.5 + 8

* Microsections made on 'Area A' after 181 d

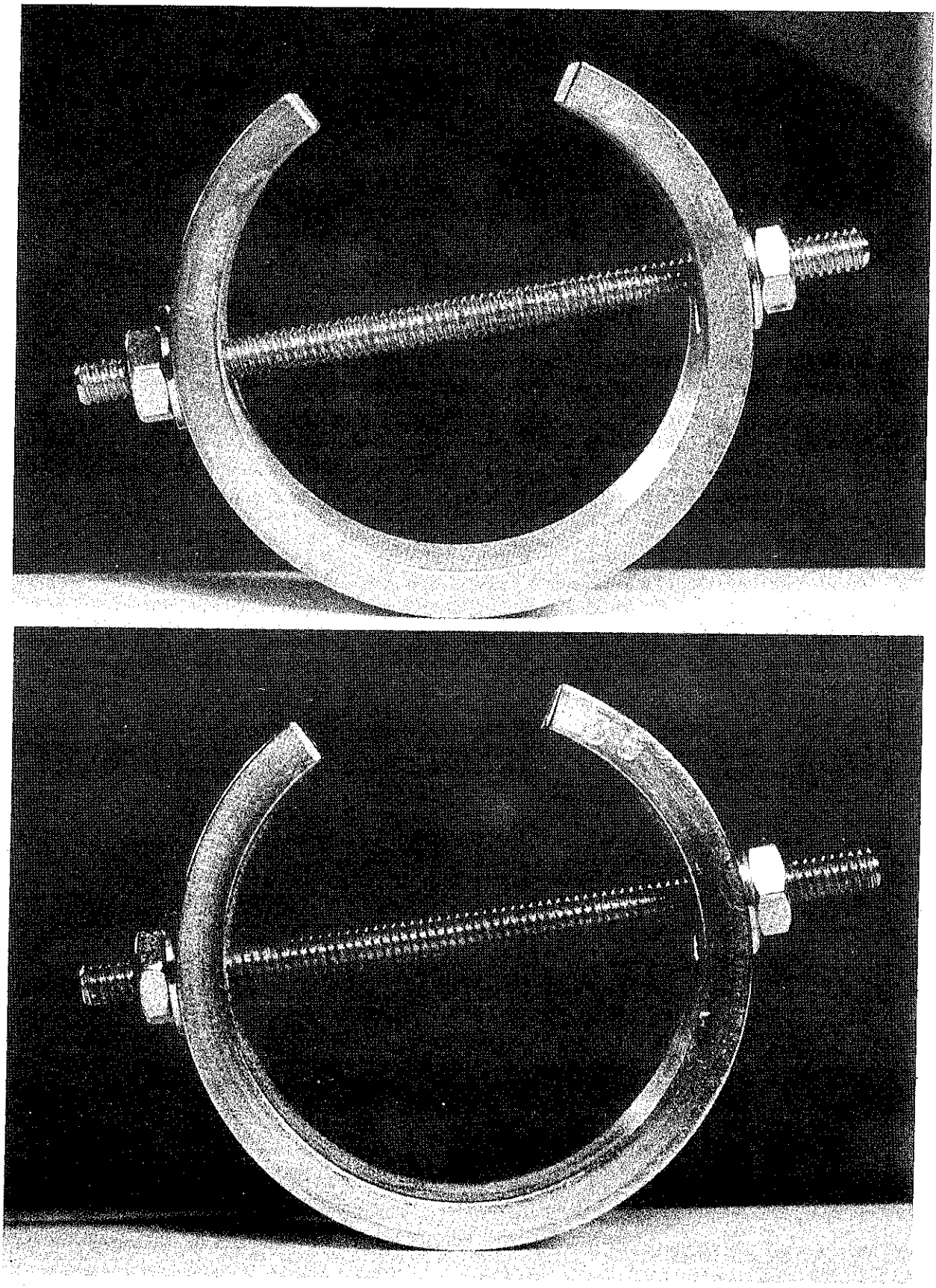

Figure 2. Photographs of C-ring samples 4 (upper) and 35 (lower)

2.5.2 *Inspection*

The initial inspection was performed three days after the C-rings had been loaded to the required stress levels. Six further detailed inspections have since been made.

The entire inside surface of each specimen was inspected in turn and observations recorded on log sheets. The inner surfaces of the C-rings were divided into three zones, each possessing different levels of compressive plating stress. These zones, A, B and C, of the specimen quadrant are illustrated above Table 3. This table records the nominal stress levels within each zone, for each specimen type (e.g. specimens having zero, intermediate and high stress ranges).

A practical problem for all experiments seeking to pin-point nucleation sites and calculate the growth rates of whiskers on a large number of different specimens over long periods, is that surface morphologies must be continually recorded by microphotography at several magnifications and this requires several hundred individual photographs. The major inspections were made over six periods of time. Four critical inspection points were made with a Jeol JSM-U3 model SEM using a specially constructed jig into which individual C-ring specimens could be placed. The jig was centred at the rotational axis of the specimen stage. Each specimen could be rotated with the electron beam, continually focussed, scanning the inside wall surface. This allowed high-definition photomicrographs to be made in all the preselected areas. The jig facilitated the recording of rotational angles, so that identical areas could be relocated after further storage periods.

2.5.3 *In-situ analysis of composition*

Point analyses were made of the plated C-ring surfaces, the nodules and the whiskers that were present at the end of the test period. These were made with a KEVEX energy-dispersive X-ray micro-analysis attachment to the SEM. In order to achieve quantitative analytical results, the instrument settings were kept constant.

Graphs of the spectra were printed from a computer disk memory.

2.5.4 *Metallography*

The small portion of unstressed C-ring that terminates as the open segment in Figure 2 was selected for metallography. One piece from each set of specimens

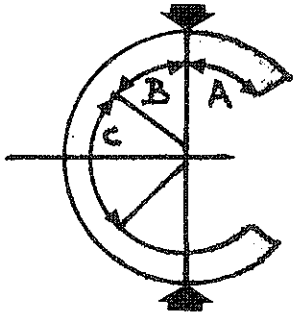

DENOTED C-RING STRESS LEVEL	COMPRESSIVE STRESS LEVELS* ON INTERNAL SURFACE AREAS		
	A	B	C
'None'	0	0	0
'Slight'	0	0→ 3.5	3.5→ 5.0
'High'	0	0→28.3	28.3→40.0

* By calculation, in kg/mm^2.

TABLE 3. *Resultant compressive stresses in tin plate caused by deflection of C-rings*

was carefully removed at the end of the test period with a jeweller's saw. These pieces were mounted in a low exothermic resin and transversely sectioned so as to expose the true plating thickness. The polished mounts were selectively etched, examined and then photographed.

2.5.5 Evaluation of intermetallic growth

Small unstressed portions, similar to those utilised for metallography, were placed in a specially constructed tin stripping cell. The samples were attached to gold-plated nickel conductors and positioned to face a sheet of lead at a distance of 50 mm. The electrolyte was made up from 20 g sodium hydroxide pellets in 1 l of distilled water. With a sample electrically connected as the cathodic element, tin was slowly stripped from the plated C-ring surfaces (0.2 A per 25 mm^2 sample surface area, at approximately 4 V).

Once the tin had been removed from each specimen, the newly exposed surfaces were submitted to SEM examination.

2.6 EVALUATION OF STRUCTURE AND GROWTH DIRECTIONS

2.6.1 X-ray diffraction

Several long whiskers were removed from both substrates (tin-plated steel with copper barrier layer, and tin-plated brass). They were submitted to crystallographic examination by X-ray diffraction using an oscillation camera (often referred to as the Rotating Crystal Method).

With the aid of a binocular microscope, individual whiskers were glued to the pointed ends of quartz glass needles by means of a fast-setting epoxy resin. Before the resin hardened, the orientation of each whisker was improved by judiciously pushing it with a plastic pointer, so that each whisker's longitudinal axis protruded, in line from the quartz needle, a distance of about 0.5 mm. The quartz needle was then placed on the goniometer of the oscillation camera and correctly positioned such that the whisker would lie within the incident beam of X-radiation to be emitted by the collimator.

The whiskers were oscillated through 10° about the axis of the goniometer and exposed to a beam of Cu K α radiation at 40 kV and 20 mA. The collimator had a diameter of 1 mm.

The very small diameter and low mass of these

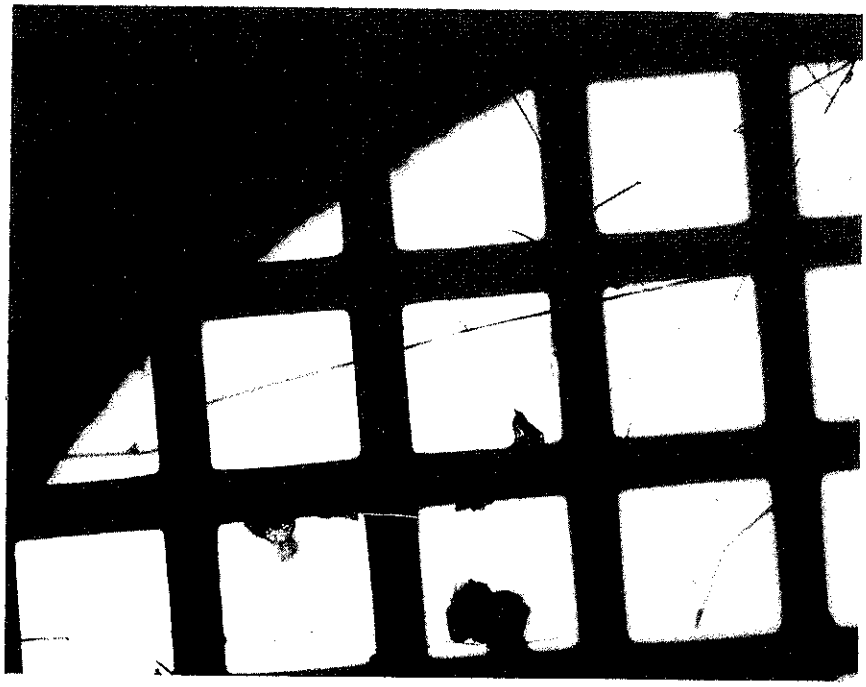

Figure 3. Appearance of whiskers subjected to TEM (after ion bombardment) (×250)

whiskers necessitated long exposure times of 24 h per sample. The film attached to the inside wall of the camera's cylindrical holder was removed daily and replaced by a new film for the following whisker exposure. Each film was developed, dried, and examined on a viewing screen.

2.6.2 Transmission electron microscopy

The application of the Transmission Electron Microscope (TEM) to metallurgical investigations has become widespread. Unfortunately, this technique has some severe limitations when applied to tin samples.

It was considered that whiskers of tin, having diameters not exceeding 2 μm should be completely transparent to the normal operating accelerating voltages of a 200 kV TEM. Preliminary trials on such whiskers (0.5−2 μm diameter) attached to grids were unsuccessful and transmission was not achieved.

It became apparent that even the thinnest of the whiskers harvested from the steel housing and the C-ring samples would require thinning by some form of preparation. After several trials with electrolytic polishing and ion etching, some long whiskers were noted to have portions totally removed; after ion bombardment they tapered down to very fine wedges, as is shown in Figure 3.

Grids supporting ion-etched whiskers were examined with the aid of a standard 200 keV TEM and a very modern high-voltage electron microscope (1 MeV).

2.6.3 Allotropic transformation

Most reference books state that when the temperature of white tin is lowered to below 13 °C, this phase can be transformed to a powder-like state that is cubic in structure and known as grey, or alpha tin. The alpha phase forms spontaneously if white tin is kept below the 13 °C transition temperature for a sufficiently long time. (According to the Tin Research Institute, this transformation can take from anything from hours to years and is dependent upon impurity levels, the hold temperature, the sample stress levels and the presence of grey tin dust to act as an inoculator [7]).

Samples of white tin whiskers were taken from the various C-ring specimens. They were glued, stress free, onto solid brass cylinders. After an initial inspection by scanning electron microscopy, they were suspended in a dewar flask, some samples being immersed in liquid nitrogen (at −196 °C) and others held in the evolving gaseous nitrogen at a temperature of between −50 and −30 °C. These samples were re-examined after different times of exposure, varying from 0.5 h to 168 h. The brass sample holders were transferred rapidly from the cryogenic environment into the SEM specimen housing, which was immediately evacuated. The large thermal mass of the sample holders, together with the absence of thermal convection within the SEM chamber, ensured that each whisker would be examined below its theoretical transition temperature, i.e. any surface morphological changes caused by the beta-to-alpha transformation should be detectable.

3. RESULTS

3.1 RESULTS OF VISUAL AND SEM INSPECTIONS

Tin whiskers have been observed to nucleate and grow from the majority of the as-plated C-ring surfaces. The nucleation period prior to growth was short for those tin platings that had been applied either directly onto a brass substrate or onto a copper intermediate layer. The 'normal' commercial tin plating was observed to support the largest initial rates of growth, followed by the 'abnormal' high-current-density tin-plating. The length of these whiskers was in excess of 0.5 mm after a shelf life of only two months. The organically contaminated platings were slow to nucleate whiskers. The 'normal' tin-plating made directly to the mild steel substrates incurred extremely long nucleation periods of approximately 6 months, whereas the 'abnormal', 'contaminated' or fused tin platings made to mild steel were not observed to support any signs of whisker growth.

Tables 4 to 8 list the detailed results of whisker-length measurements made under optical and SEM inspection at each of the stated test durations. The population densities are not recorded in tabular form owing to the great variations noted at each field of view. This aspect will be described later, in conjunction with an account of the topographical features.

The tabulated results strongly indicate that the several ranges of compressive stress levels imposed on the platings by the deflection of the C-rings have no influence on either the subsequent whisker nucleation times or the propensity for whisker growth. In excess of 250 photomicrographs were made of whiskers growing on areas under different stress. No morphological differences were observed between zero stress and maximum stress zones. Consequently, the whisker growths presented here will usually be limited to 'Area B' of the first specimen in each triplicated test series.

The mechanism for stressing each C-ring specimen (Fig. 2) relies on the torque loads applied to the stainless-steel retention nuts. High levels of compressive force are transmitted to the thin tin-plating sandwiched between each washer and the C-ring substrate. It is interesting to note the absence of preferential whisker-growth sites either beneath or immediately around the retaining nuts and washers.

The extensive depth of focus provided by the SEM has recorded a series of truly remarkable topographical features. A number of the more interesting SEM photomicrographs are included as Figures 4–15. Detailed descriptions of the many surface features are given in the captions to these figures.

The morphological features can be summarised as follows. The tin whiskers range in diameter from 6 nm to 6–7 μm, and they are usually characterised by the presence of striations parallel to their growth direction. Several of the higher-magnification photomicrographs suggest that these striations may be related to the shape of the surface orifice through which they seem to be extruded. Occasionally, whiskers have very irregular growth directions and odd changes in cross-sectional areas. Most whiskers extend up from gross eruptions termed 'nodules', but it would appear that if nodules are not present during the initial period of growth, then nucleation of whiskers will be delayed. Also, whiskers having a long nucleation period may appear to have a pyramid-, or pointed-needle-like shape. Whisker growth is accompanied by a rotation of the shaft about an axial line drawn normal from the nucleation point on the tin-plated surface. This rotation or gyratory movement can cause whiskers with low projection angles to become entangled with other whiskers or nodules.

The whisker population density varies from one specimen to another, but is generally 5–300 mm^{-2} on those surfaces supporting growths.

3.2 COMPOSITION OF PLATINGS AND WHISKERS

The results of the surface analyses made on the various C-ring specimens and their whiskers are presented in Table 9. These quantitative results were made possible by ensuring that the KEVEX EDAX instrument settings were kept constant throughout the analysis. These results were taken at the 634 d inspection period. Qualitative EDAX analyses had been made under low-energy electron bombardment at the onset of the programme, when all specimens were noted to support pure tin-platings.

A review of Table 9 shows specimen 3 to give an unusually high result for zinc. This value was provided from a computerised calculation, but it was confirmed by the spectrum display. The topography and microsection of this sample (Fig. 4) does not account for this anomaly. All other analytical results are in

keeping with the physical and morphological properties of the C-ring specimen. The following notable observations can be made:

- Appreciable amounts of zinc have diffused from the brass substrate to the tin surface during the course of the experiment. This is particularly true for the 'normal' tin, and less marked for the 'abnormal' tin platings. Copper was also detected, but appears to be less mobile than zinc.
- The nodules present on tin-platings made directly to brass C-rings are composed mainly of tin with additions of zinc and copper.
- A copper intermediate layer acts as a barrier to zinc diffusion from the brass substrates.
- The tin fusion (melting) process has caused an increase in the amount of copper (and possibly zinc) on the brass C-ring surfaces.
- The surface of tin plated directly to the steel substrate remained as 100% pure tin. No iron was detected.
- The steel C-rings that had been copper-plated prior to the tin finish revealed evidence of surface copper at the end of the storage period.
- The amount of surface copper present on the steel sample that had a fused tin plating was high and of the same order as for fused tin on the brass substrates.
- Whiskers growing from tin-plated brass substrates are composed mainly of tin with approximately 2% by weight of zinc, but no copper.
- Whiskers growing from tin-plated steel specimens having a copper intermediate layer are composed of pure tin.

3.3 METALLOGRAPHY

Transverse microsections were made across the unstressed overhanging portion of the C-rings as described in Section 2.5.4. In several cases these cross sections dissected nodules and whiskers.

Accurate measurements of plating thickness were made for each internal C-ring specimen surface by inspection of the microsections. These results have been incorporated alongside the nominal thickness in Table 2. A review of this table reveals some deviations from the designed plating thickness. The copper intermediate layers, when present, were thinner than expected (maximum deviation being 1.5 μm). The tin platings were required to be 5 μm thick, but did in fact range from 3 to 8 μm. The various plating procedures used in the preparation of the samples account for these thickness variations, as each bath set-up will have a different 'throwing power' (i.e. the property of the plating solution to deposit the required thickness of tin plating onto the inside (recessed) surface of the C-ring).

For the purpose of the experimental results, no distinction is made between the different specimens, the deviations from nominal thickness being considered small in comparison with the very wide range of tin-plating thicknesses found on commercial electronic products (which can range from 1 to 25 μm).

An attempt was made to measure the thickness of the intermetallic compound layer on the screen of the projection microscope at magnifications of 1000× and 1500×. The theoretical minimum resolvable distance of 0.3 μm under ideal conditions precluded any accurate measurements. Evidence of a light-coloured compound was established at both the brass- and the copper-to-tin interfaces. The intermetallic appeared as a series of irregular growths, reaching a thickness of about 0.4 μm on the brass C-ring. The copper intermediate plating supported a continuous intermetallic layer between 0.2 and 0.4 μm thick.

The topography of the intermetallic compound layer was revealed by SEM inspection of the cathodically stripped C-ring segments.

A selection of these layers is illustrated in Figures 16–18. They confirm some of the metallographic observations:

- the presence of only one intermetallic layer (i.e. Cu_6Sn_5);
- the fact that the intermetallic is very thin and present as an *irregular* growth on the *brass* substrate and as a *continuous* layer on the *copper* plate.

It seems certain that the tin nodules and whiskers are intimately attached to the underlying intermetallic layer, as they were not removed by several seconds of immersion in an alcohol-filled ultrasonic cleaning bath.

3.4 GROWTH RATES

An attempt is now made to estimate the average rates of growth of the *longest* whiskers, which can be expected to account for most problems involving actual short-circuits in electronic equipments.

Tables 4–7 have been collated into a summarised form in Table 10. These values are expected to provide the maximum whisker growth rates that occurred during the time span of the experiment. They are presented in graphical form in Figures 19–21. These logarithmic plots do not purport to detail the growth of individual whiskers against time and hence they cannot be used for any accurate diagnostic analysis of the whisker-growth mechanism. However, it is evident that each curve displays, to some degree, three stages of whisker development:

(a) nucleation period
(b) period of growth
(c) reduction and termination of growth.

It is noted from a previous observation that the application of various levels of compressive stresses to the tin-plated C-ring samples has no influence on the nucleation period or rate of whisker growth. In addition, the following assumptions are derived from Figures 19–21:

3.4.1 Nucleation period

Both 'normal' and 'abnormal' tin platings made directly to brass, copper-plated brass and copper-plated steel can possess very short (within 2 d) nucleation periods prior to whisker growth. Under the same substrate conditions, the organically contaminated tin plating possesses a longer nucleation period of between 3 and 30 d. Normal tin plated directly to steel possesses a long nucleation period that exceeds 100 d, whereas the other forms of tin plated to steel have yet to nucleate whiskers (after 1269 d of storage). With the exception of specimen No. 40, which nucleated some short whiskers after 1269 d, the fused tin coatings do not support growth.

3.4.2 Growth period

Figures 19–21 indicate that the growth period for the longest whiskers generally lasts in the order of 200 d. However, whiskers growing on tin plated directly onto the steel C-rings are still continuing to grow and cannot be fully assessed. It was also noted, from the recent SEM inspections, that whereas the long whiskers appear to have terminated their growth, additional whiskers (i.e. those with a needle-like or pyramidal shape) continue to nucleate and grow.

The rates of growth are given by the slopes of tangents drawn to the curves in Figures 19–21. In many instances these curves approximate a straight line (i.e. linear-time growth occurs directly after nucleation of the whisker). There appears to be little or no correlation between rate of growth and type of plating or substrate. Calculations show that, once nucleated, whiskers can grow at rates between:

0.029 nm/s (minimum observed)

and

0.230 nm/s (maximum observed).

3.4.3 Termination of growth

Several of the SEM views of growing whiskers demonstrate growth to be accompanied by a rotation or gyration of the whisker shaft. Termination of growth can be demonstrated by an absence of whisker movement and this has been documented after a growth period of approximately 200 d for the longest whiskers seen on the C-ring specimens [for examples, see photographs (ii) and (iii) of Fig. 8, or (b) and (d) of Fig. 13].

3.5 STRUCTURE AND GROWTH DIRECTIONS OF TIN WHISKERS

3.5.1 X-ray diffraction results

Preliminary trials indicated that long exposure times would be necessary to achieve a reasonably clear set of diffraction photographs for the various whiskers selected for investigation. Optimum results were achieved with a collimator aperture opening of 1 mm diameter and an exposure period of 24 h. Five of the eight whiskers submitted to crystallographic evaluation produced diffraction patterns suitable for evaluation and characterisation.

The most obvious feature of the resulting diffraction photographs was the sets of parallel straight lines of

spots. Fortunately, a zone axis of each of the five whiskers coincided with the camera's oscillation axis and produced clear horizontal rows of spots displaying much symmetry. These reflections, or lines of spots are termed 'layer lines'. The spots on the central layer line are reflections from planes whose normals are in a horizontal plane; the spots on the other layer lines are from planes that have the same intercept on the axis of oscillation.

The whisker's unit-cell parameters, lattice spacings and indexing were calculated by recording the coordinates measured for each of the spots on the oscillation photograph. White tin has a tetragonal crystal structure with lattice constants of $a=5.831$ Å and $c=3.182$ Å at 26°C. The density is 7.285 g/cm^3 at 18°C. The elementary cell contains nine atoms as sketched in Figure 22.

A typical diffraction pattern for Sample 2 is included as Figure 23; it is accompanied by the detailed measurements and calculated results for individual unit-cell parameters and, for information, their Miller indices. Darkening in the centre of these films results from very long exposure times (spots in the dark region are only visible when each film is illuminated on a viewer). The shortest unit-cell parameters, or translations t, were determined from the photographs, with the following results*:

Sample	Shortest t	Growth direction
Tin-plated copper on steel (C-ring specimen No. 35)		
2	6.64 Å = $t3$	[101]
3	6.64 Å = $t3$	[101]
4	5.88 Å = $t1$	[100]
Tin plated on brass (specimen unknown)		
5	3.18 Å = $t2$	[001]
	5.84 Å = $t1$	[100]
6	4.45 Å = $t4$	[111]

* NOTE: The nomenclature is explained in Figure 22.

The second-layer lines of whisker sample 5 were separated from the central line by a distance unequal to any multiple of the distance from the first-layer lines. This demonstrates that sample 5 consists of two different single crystals. Examination of this whisker with the Reichert microscope at a magnification of ×400 indicated the presence of a short straight whisker segment situated between two kink bands. Similar marks were not seen on the other whiskers.

These crystallographic determinations are in agreement with those presented 25 years ago by Ellis, Gibbons and Treuting [8]. The growth directions are of small crystallographic indices and they appear to be independent of the 'tin-plated substrates' composition. The unit-cell parameters are found to be very close to the theoretical parameters for single crystal tetragonal beta tin, and this tends to confirm the absence of major impurity atoms from the whiskers' crystal structure.

3.5.2 Results of TEM work

An optical view of a completely thinned whisker is shown in Figure 3. This specimen proved to be relatively transparent to the electron beam of the 200 keV TEM and produced the composite images shown in Figure 24. The thin section shown in this figure includes an extremely thin air gap, which is expected to be the location of one of the characteristic flutes that decorate the shafts of most whiskers. Thinning has unfortunately not been uniform, and areas of the sample support micropeaks and troughs. Most edges have a ragged appearance. The sharp edge of the wedge is completely fragmented.

Many micrographs were made of the edges of different whisker foils. Each figure recorded: (a) the local bright field image, and (b) its diffraction pattern. The aperture of the TEM was then aligned (off-axis) with one of the diffracted beams so as to produce a dark field image (c). From an evaluation of the results, one can draw the following conclusions:

- All micrographs show thickness fringes (in both bright and dark fields). These are sample preparation characteristics and are not related to microstructure effects.
- No forms of grain boundaries are observed.
- No dislocations, stacking faults or loops that might have expanded to form surface twins are recorded.
- Second phases are not observed.
- Elastic strains are not present as the diffraction points are circular and not elongated.

It should be noted that each whisker investigated by TEM existed as a straight length. None of the sharp bends or kink formations occasionally present on growing whiskers could be isolated for examination.

3.5.3 Allotropic transformation

Approximately 100 whiskers have been subjected to cryogenic temperatures. The hold times for exposure to both liquid and gaseous nitrogen ranged from 0.5 to 168 h, after which time the samples were rapidly transferred to an SEM and examined whilst still at a temperature below that theoretically required to cause the white-to-grey allotropic transformation of tin.

It is known that if a compact polycrystalline piece of white tin is transformed, a powdery mass possessing cracks will slowly result. The transformation is accompanied by a large increase in volume (27%) [9]. Grey tin has been reported to convert back to white tin once the temperature is raised above the equilibrium temperature, but only when compact pieces of grey tin exist as the starting material.

Despite many repeated and careful examinations of the cryogenically exposed tin whiskers, none could be seen to have acquired a changed surface morphology. All samples had retained their characteristic appearances.

According to an early paper [10], the atomic mechanism underlying the transformation has not been established, but observations seem to indicate that it is of the diffusionless or martensitic type. In white tin, which has undergone no previous transformation, a small number of nuclei are formed after a long nucleation period and the grey phase spreads out spherically around each nucleus. In white tin that has already been subjected to transformations, a limited number of nuclei are formed in every particle [10].

The negative results observed in this present work tend to indicate that the unstressed and defect-free status of tin whiskers either greatly retards or completely suppresses the allotropic transformation.

TABLE 4. *Growths on tin-plated brass substrate*

SPECIMEN NO.	TYPE OF TIN	STRESS LEVEL (Table 3)	INSPECTION PERIOD (d) LENGTH OF WHISKERS (μm)						
			(V)3	(S)27	(S)57	(V)142	(S)181	(S)634	(S)1269
1	NORMAL	NONE A	0	20	100	500	1000	1000	1000
		B	0	20	700	500	1200	1200	1200
		C	0	20	500	1000	1500	1500	1500
2		SLIGHT A	20	0	50	100	1000	1000	1000
		B	0	0	0	300	1000	1000	1000
		C	0	0	70	300	1500	1500	1500
3		HIGH A	0	0	50	100	200	200	200
		B	0	0	20	100	200	600	600
		C	0	0	100	100	150	250	250
4	ABNORMAL	NONE A	0	0	35	0	50	50	50
		B	0	50	120	100	150	150	150
		C	0	0	0	0	10	10	10
5		SLIGHT A	0	0	35	30	50	50	50
		B	20	20	100	100	100	100	100
		C	0	0	10	0	50	50	50
6		HIGH A	0	0	60	0	200	200	200
		B	0	0	50	100	600	600	600
		C	0	0	10	0	10	10	10
7	CONTAMINATED	NONE A	0	0	0	0	60	80	80
		B	0	0	0	0	0	0	1600
		C	0	0	0	0	50	50	200
8		SLIGHT A	0	0	0	0	180	180	1200
		B	0	0	0	0	100	100	400
		C	0	0	0	0	0	0	400
9		HIGH A	0	0	0	0	1000	1000	1000
		B	0	0	10	0	200	200	200
		C	0	0	0	0	100	100	100

(V) = Visual inspection at 80× magnification
(S) = SEM inspection

TABLE 5. *Growths on tin-plated brass with copper barrier*

SPECIMEN NO.	TYPE OF TIN	STRESS LEVEL (Table 3)	INSPECTION PERIOD (d) LENGTH OF WHISKERS (μm)						
			(V)3	(S)27	(S)57	(V)142	(S)181	(S)634	(S)1269
10	NORMAL	NONE A	50	50	120	100	300	300	300
		B	0	150	50	50	300	300	450
		C	50	100	100	100	300	300	300
11		SLIGHT A	50	200	500	500	500	500	500
		B	50	100	140	200	600	600	600
		C	50	50	60	100	100	100	100
12		HIGH A	0	20	20	0	50	50	450
		B	0	0	10	0	50	50	50
		C	0	0	0	0	50	50	50
13	ABNORMAL	NONE A	0	0	100	100	150	200	200
		B	0	0	350	100	700	700	700
		C	0	0	10	0	10	10	10
14		SLIGHT A	0	0	260	200	280	280	280
		B	0	0	300	300	300	300	300
		C	0	0	10	0	10	10	10
15		HIGH A	50	300	600	600	1100	1100	1100
		B	0	100	400	400	450	450	450
		C	0	100	300	300	600	600	600
16	CONTAMINATED	NONE A	0	0	0	0	40	60	100
		B	0	0	0	0	40	40	50
		C	0	0	0	0	40	40	50
17		SLIGHT A	0	0	0	0	200	200	200
		B	0	0	0	0	40	40	140
		C	0	0	0	0	40	40	40
18		HIGH A	0	0	0	0	20	20	20
		B	0	0	10	0	100	100	140
		C	0	0	0	0	40	40	40

(V) = Visual inspection at 80× magnification
(S) = SEM inspection

TABLE 6. *Growths on tin-plated steel substrate*

SPECIMEN NO.	TYPE OF TIN	STRESS LEVEL (Table 3)	INSPECTION PERIOD (d) LENGTH OF WHISKERS (μm)						
			(V)3	(S)27	(S)57	(V)142	(S)181	(S)634	(S)1269
21	NORMAL	NONE A	0	0	0	0	10	10	10
		B	0	0	0	0	10	10	20
		C	0	0	0	0	10	10	10
22		SLIGHT A	0	0	0	0	10	10	10
		B	0	0	0	0	10	10	10
		C	0	0	0	0	10	10	10
23		HIGH A	0	0	0	0	0	0	10
		B	0	0	0	0	0	0	15
		C	0	0	0	0	0	0	0
24	ABNORMAL	NONE A	0	0	0	0	0	0	0
		B	0	0	0	0	0	0	0
		C	0	0	0	0	0	0	0
25		SLIGHT A	0	0	0	0	0	0	0
		B	0	0	0	0	0	0	0
		C	0	0	0	0	0	0	0
26		HIGH A	0	0	0	0	0	0	0
		B	0	0	0	0	0	0	0
		C	0	0	0	0	0	0	0
27	CONTAMINATED	NONE A	0	0	0	0	0	0	0
		B	0	0	0	0	0	0	0
		C	0	0	0	0	0	0	0
28		SLIGHT A	0	0	0	0	0	0	0
		B	0	0	0	0	0	0	0
		C	0	0	0	0	0	0	0
29		HIGH A	0	0	0	0	0	0	0
		B	0	0	0	0	0	0	0
		C	0	0	0	0	0	0	0

(V) = Visual inspection at 80× magnification
(S) = SEM inspection

TABLE 7. *Growths on tin-plated steel with copper barrier*

SPECIMEN NO.	TYPE OF TIN	STRESS LEVEL (Table 3)	INSPECTION PERIOD (d) LENGTH OF WHISKERS (μm)						
			(V)3	(S)27	(S)57	(V)142	(S)181	(S)634	(S)1269
30	NORMAL	NONE A	0	100	220	200	600	600	600
		B	20	100	100	300	400	400	400
		C	0	0	50	50	300	300	300
31		SLIGHT A	0	50	200	200	250	250	250
		B	0	1000	225	200	300	300	300
		C	0	20	100	100	100	100	100
32		HIGH A	0	200	400	400	500	500	500
		B	0	100	300	300	400	400	400
		C	0	100	500	500	500	500	500
33	ABNORMAL	NONE A	0	100	20	100	600	600	600
		B	0	300	20	0	220	220	220
		C	0	0	20	0	100	100	100
34		SLIGHT A	0	500	800	800	800	800	800
		B	0	0	50	50	50	50	50
		C	0	50	50	50	50	50	50
35		HIGH A	20	500	1100	1200	1200	1200	1200
		B	0	100	425	500	600	600	600
		C	0	100	400	400	300	300	300
36	CONTAMINATED	NONE A	0	0	0	0	0	50	100
		B	0	20	40	40	40	70	400
		C	0	0	0	0	0	0	350
37		SLIGHT A	0	0	50	50	70	70	70
		B	0	20	50	50	70	70	400
		C	0	0	0	0	70	70	400
38		HIGH A	0	0	0	0	0	0	0
		B	0	20	0	0	60	80	80
		C	0	0	0	0	100	100	100

(V) = Visual inspection at 80× magnification
(S) = SEM inspection

TABLE 8. *Growths on fused tin platings*

SPECIMEN NO.	TYPE OF TIN	STRESS LEVEL (Table 3)	INSPECTION PERIOD (d) LENGTH OF WHISKERS (μm)						
			(V)3	(S)27	(S)57	(V)142	(S)181	(S)634	(S)1269
19	NORMAL Fused tin on brass substrate	HIGH A	0	0	0	0	0	0	0
		B	0	0	0	0	0	0	0
		C	0	0	0	0	0	0	0
20	NORMAL Fused tin, copper barrier on brass	NONE A	0	0	0	0	0	0	0
		B	0	0	0	0	0	0	0
		C	0	0	0	0	0	0	0
39	NORMAL Fused tin on steel substrate	NONE A	0	0	0	0	0	0	0
		B	0	0	0	0	0	0	0
		C	0	0	0	0	0	0	0
40	NORMAL Fused tin, copper barrier on steel	NONE A	0	0	0	0	0	0	0
		B	0	0	0	0	0	0	6
		C	0	0	0	0	0	0	0

(V) = Visual inspection at 80× magnification
(S) = SEM inspection

TABLE 9. *Quantitative results of the surface analysis determined for tin layer on C-ring specimens*

SPECIMEN NUMBER (and material)		ANALYSIS RESULTS (WT %)		
		COPPER	ZINC	TIN
3	(surface of normal tin-on-brass)	0.5	18.6	80.9
3	(nodule)	0.6	2.3	97.1
3	(whisker)	0.0	2.1	97.9
4	(abnormal tin-on-brass)	0.0	0.3	99.7
7	(abnormal tin-on-brass)	4.1	2.1	93.8
10	(tin-on-copper-on-brass)	0.8	0.0	99.2
13	(abnormal tin-copper-on-brass)	2.2	0.6	97.2
16	(contam. tin-on-copper-on-brass)	0.3	0.0	99.7
19	(tin-on-brass fused)	5.7	17.2	77.1
20	(tin-on-copper-on-brass fused)	8.7	2.7	88.5
21	(tin-on-steel)	0.0	0.0	100.0
24	(abnormal tin-on-steel)	0.0	0.0	100.0
27	(contam. tin-on-steel)	0.0	0.0	100.0
30	(tin-on-copper-on-steel)	1.0	0.0	99.0
33	(abnormal tin-copper-on-steel)	0.9	0.0	99.1
35W	(whisker base)	0.0	0.0	100.0
35WH	(whisker tip)	0.0	0.0	100.0
36	(contam. tin-on-copper-on-steel)	0.0	0.0	100.0
39	(tin-on-steel fused)	0.0	0.0	100.0
40	(tin-on-copper-on-steel fused)	5.3	0.0	94.7

Accuracy of results: 1% for Sn and 5–10% for both Cu and Zn.

TABLE 10. *Longest whisker growths measured on C-ring samples*

SPECIMEN TYPE	INSPECTION PERIOD (d) LENGTH OF WHISKERS (μm)						
	(V)3	(S)27	(S)57	(V)142	(S)181	(S)634	(S)1269
BRASS SUBSTRATE							
NORMAL TIN	20	20	700	1000	1500	1500	1500
ABNORMAL TIN	20	50	120	120	600	600	600
CONTAMINATED TIN	0	0	10	10	1000	1000	1600
BRASS SUBSTRATE WITH COPPER BARRIER LAYER							
NORMAL TIN	50	200	500	500	600	600	600
ABNORMAL TIN	50	300	600	600	1100	1100	1100
CONTAMINATED TIN	0	20	20	20	200	200	200
STEEL SUBTRATE							
NORMAL TIN	0	0	0	0	10	20	20
ABNORMAL TIN	0	0	0	0	0	0	0
CONTAMINATED TIN	0	0	0	0	0	0	0
STEEL SUBSTRATE WITH COPPER BARRIER LAYER							
NORMAL TIN	20	200	500	600	600	600	600
ABNORMAL TIN	20	500	1100	1100	1200	1200	1200
CONTAMINATED TIN	0	20	50	50	100	100	400

(V) = Visual inspection at 80× magnification
(S) = SEM inspection

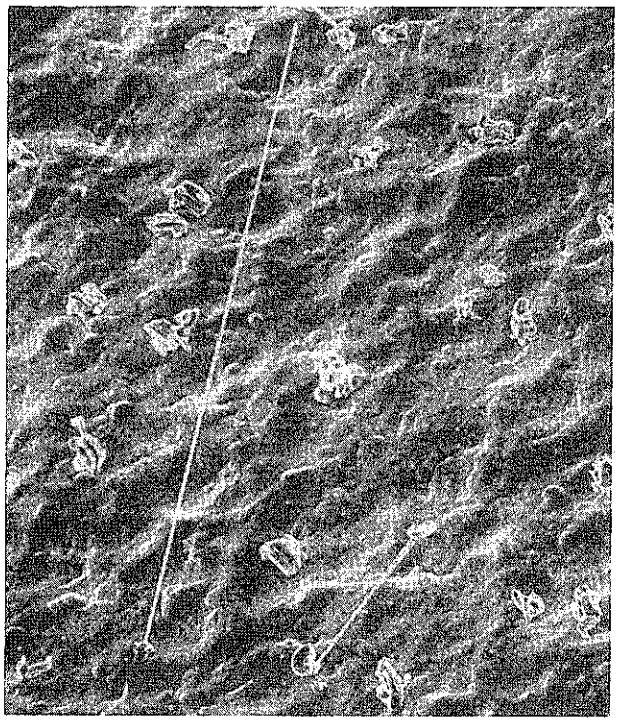

(a)

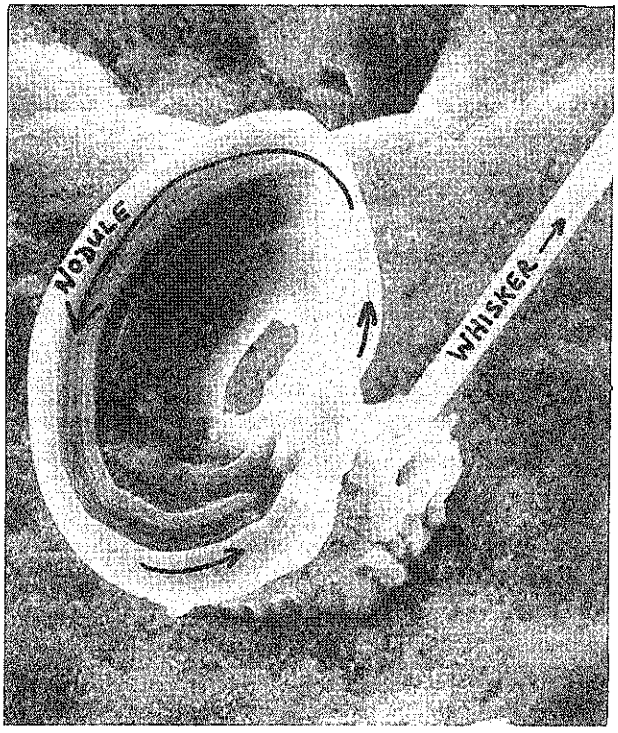

(b)

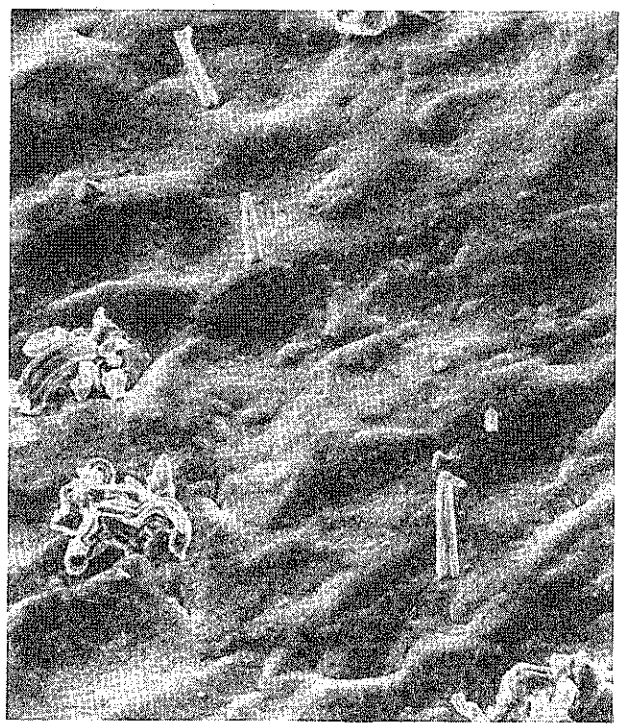

(c)

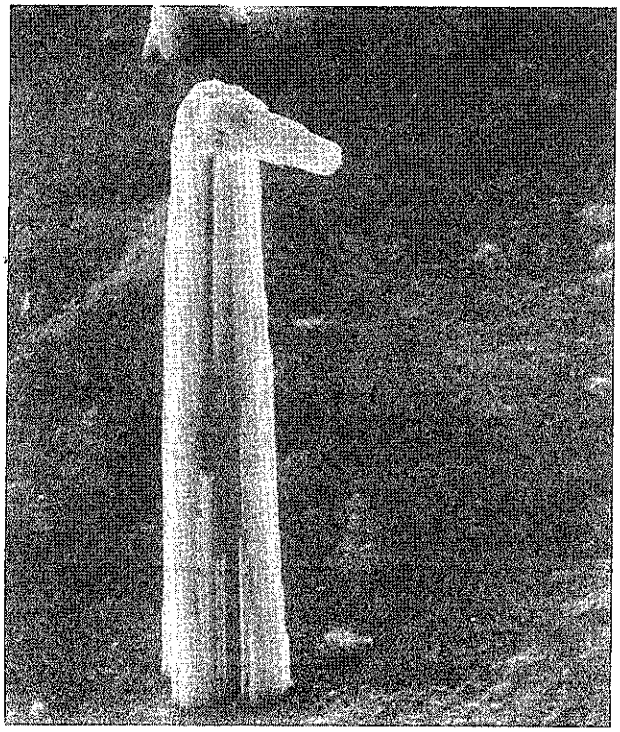

(d)

Specimen No. 1 at day 57 inspection

(a) High density of curly nodules, some associated with long whiskers (×200)

(b) Nodules appear to have been forced from the tin-plating; they have less crystallographic form than the perfectly straight 1.6 μm diameter whisker that projects from the same growth site.
This is the base of the long whisker shown in (a). (×3000).

Specimen No. 1 at day 181 inspection

(c) New protrusions of pyramid-shaped whiskers. This form of whisker has taken longer to nucleate than either the nodules or parallel sided whiskers originally photographed in (a). (×300)

(d) The pyramid shapes have more striations at their base. (×3000)

(e)

(f)

Specimen No. 3 at day 634 inspection

(e) One 0.6 mm whisker (×200).
(f) The long whisker is trapped by the pointed hook of a bent 'pyramidal' adjacent growth, arrowed on (e) (×3000).

(g)

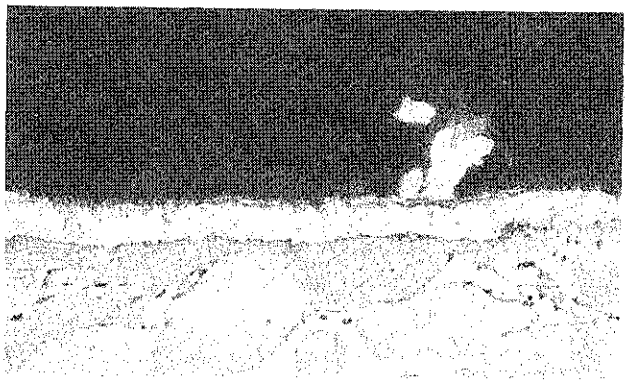

(g) Microsection shows:
tin-plating thickness is 8 μm; no subsidence by microsectioned nodule
(×600).

Figure 4. Normal tin-plated brass C-ring.

(a)

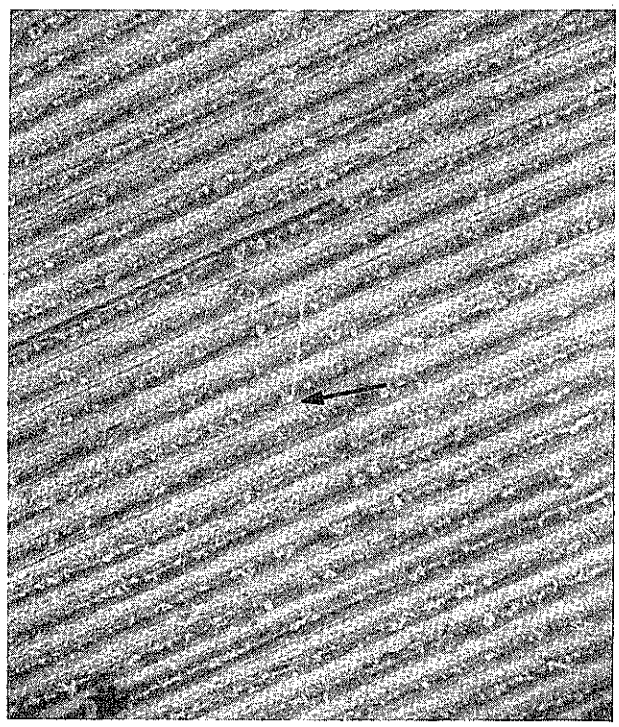

(b)

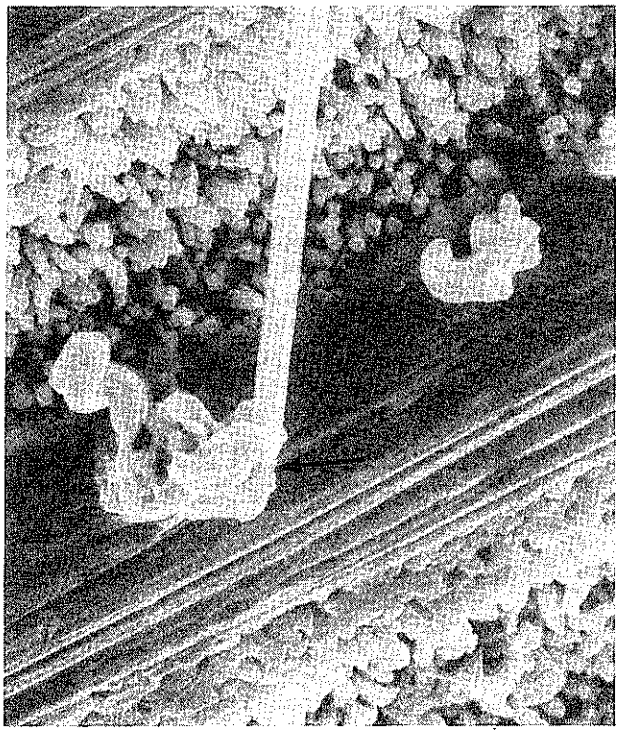

Specimen No. 4 at day 57 inspection

(a) Machine markings are clearly visible, as is the occasional whisker (×200).

(b) Growth of whisker on (a) is associated with a nodular mass (×3000).

(c)

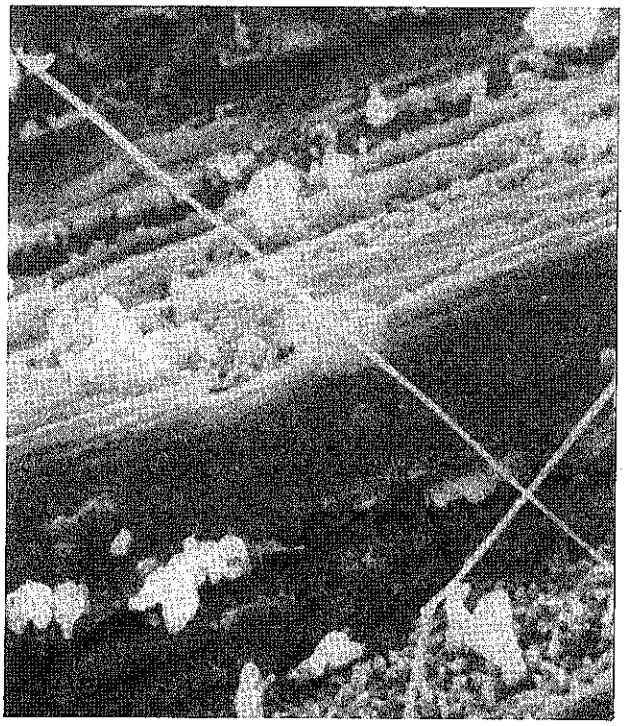

(d)

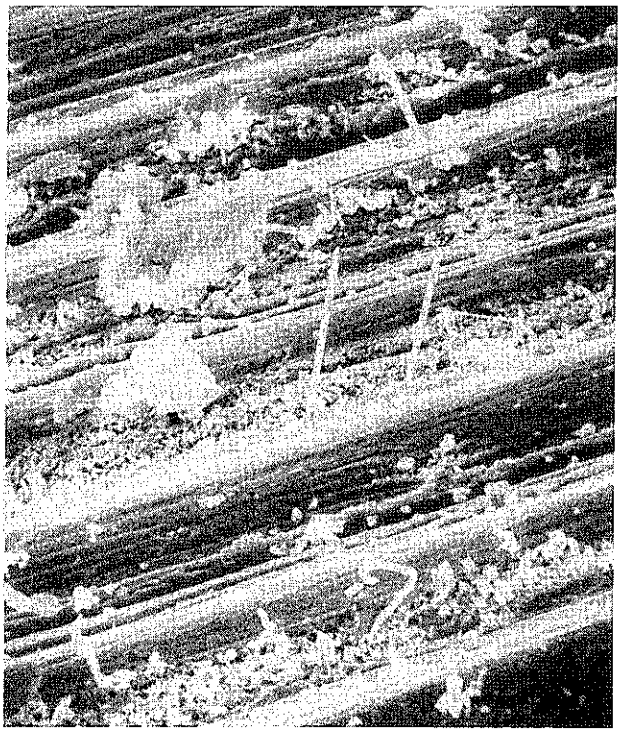

Specimen No. 4 at day 181 (c) and day 634 (d) inspection

(c) Surprisingly thin whiskers of 0.3 μm diameter (far thinner than previously recorded in the literature). (×3000)

(d) Many new whiskers of short lengths, unlike the short-nucleation-period whiskers (a)—(c), not associated with nodular extrusions. (×1000)

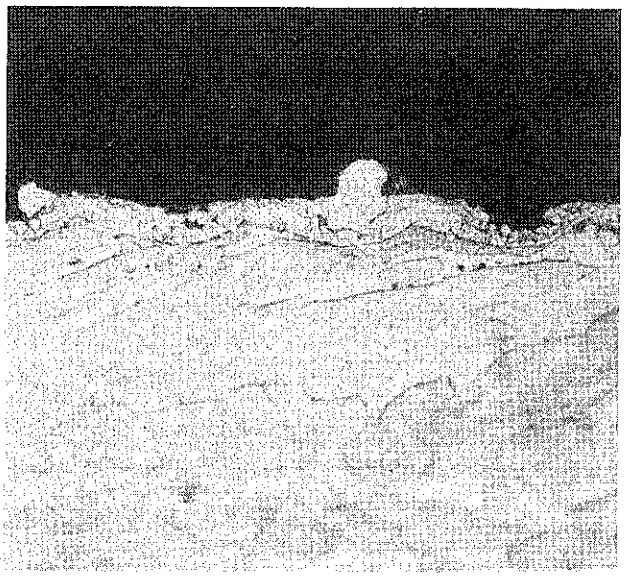

(e)

(e) Microsection shows:
Topographical machine markings can be seen in section; abnormal tin-plating does not fill all troughs. Nodules are clearly visible. Tin thickness is up to 5 μm ($\times$600).

Figure 5. Abnormal tin-plated brass C-ring.

(a)

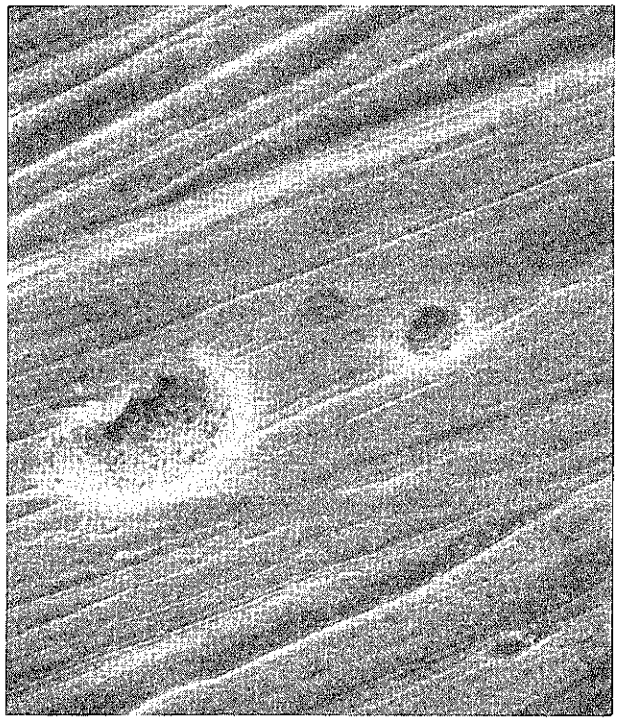

(b)

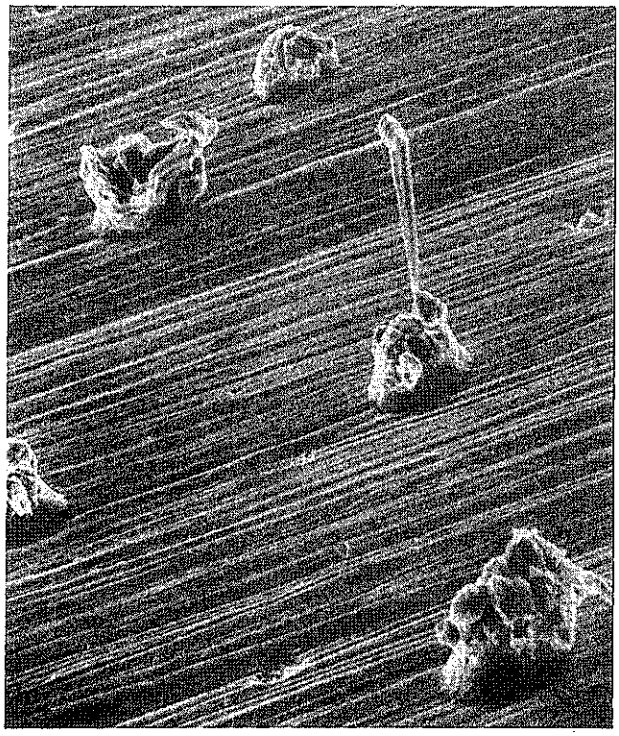

Specimen No. 7 at day 57 (a) and day 181 (b) inspection

(a) No whisker growth, but spots indicate location of particles (×3000)
(b) Small erruptions give rise to nodules and short whiskers (×200).

(c)

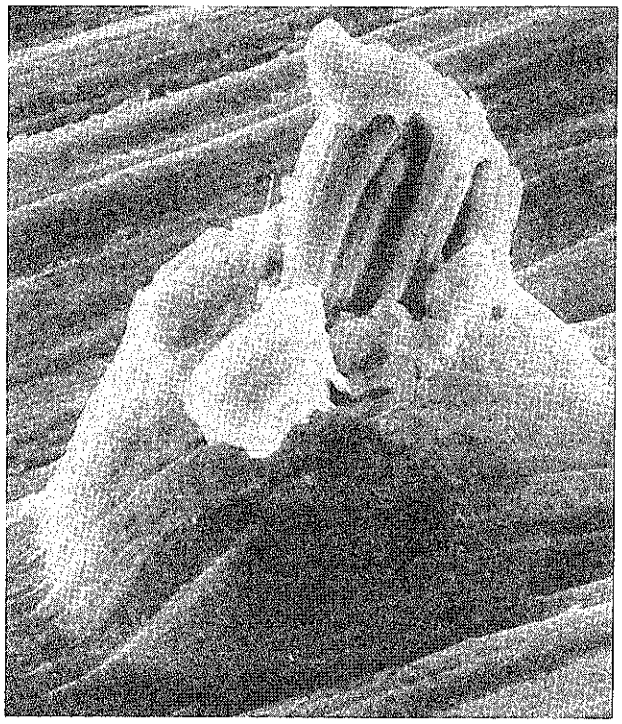

(d)

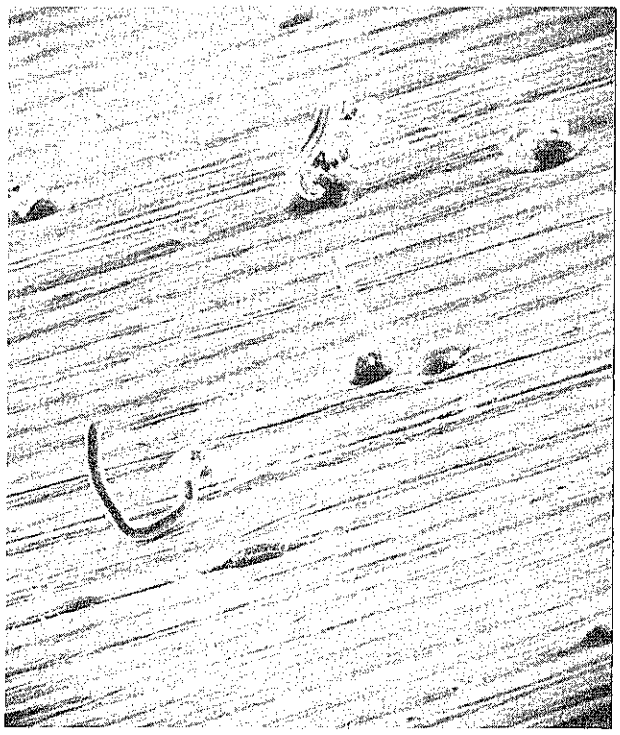

Specimen No. 7 at day 181 (c) and day 634 (d) inspection

(c) Apparent extrusion of whisker from raised hillock (×3000)
(d) Whiskers from hillocks have grown in length (×300)

(e)

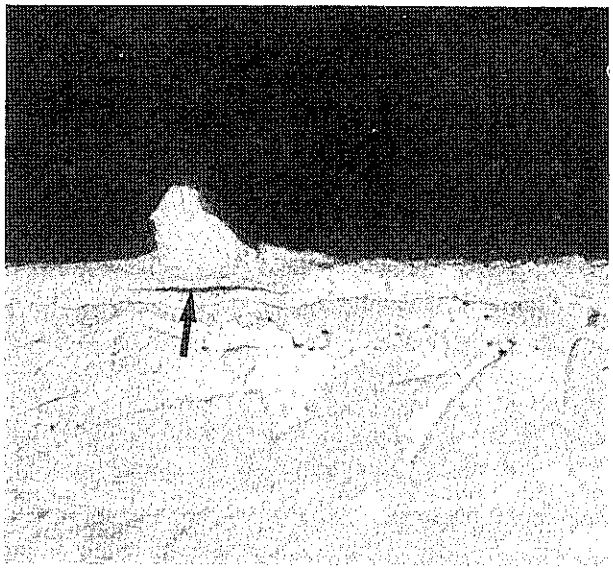

(e) Microsection features a hillock similar to that shown in (c). The morphology of an occluded organic contaminant is seen (arrowed) associated with the base of growth. (×600)

Figure 6. Organic particle contamination (flour) of pure tin-plated brass C-ring

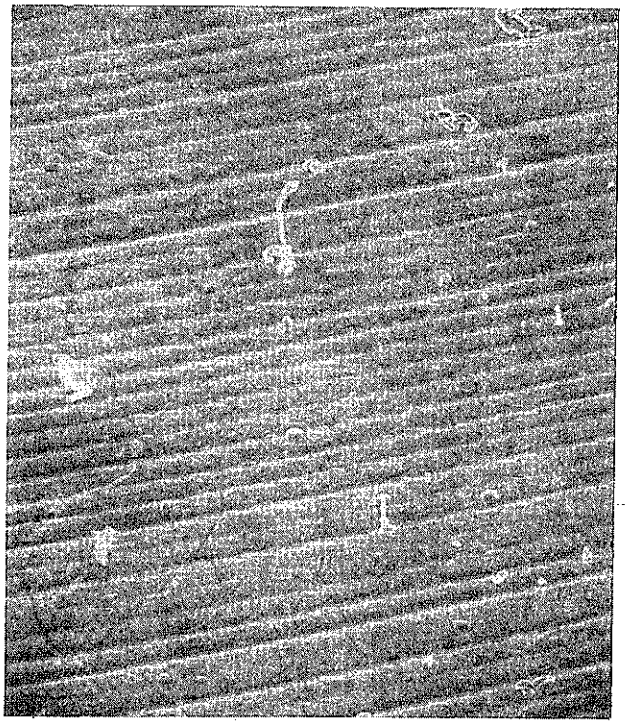

(a)

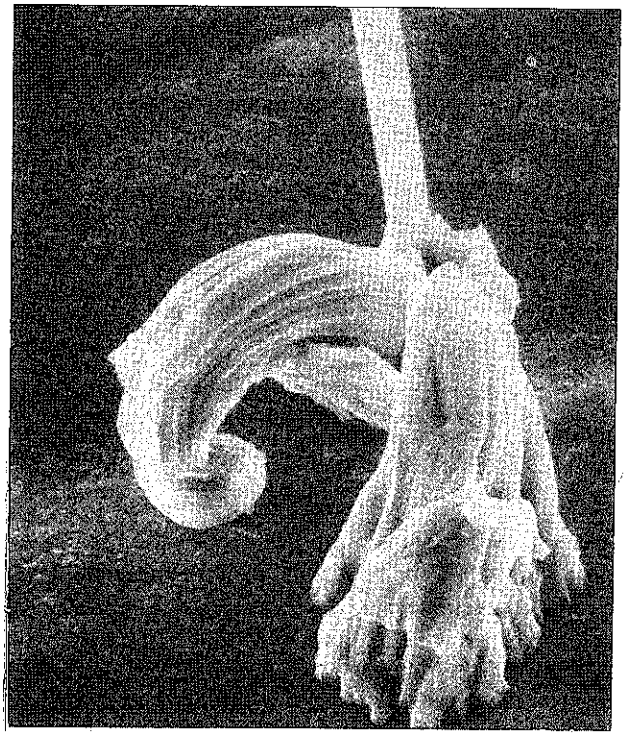

(b)

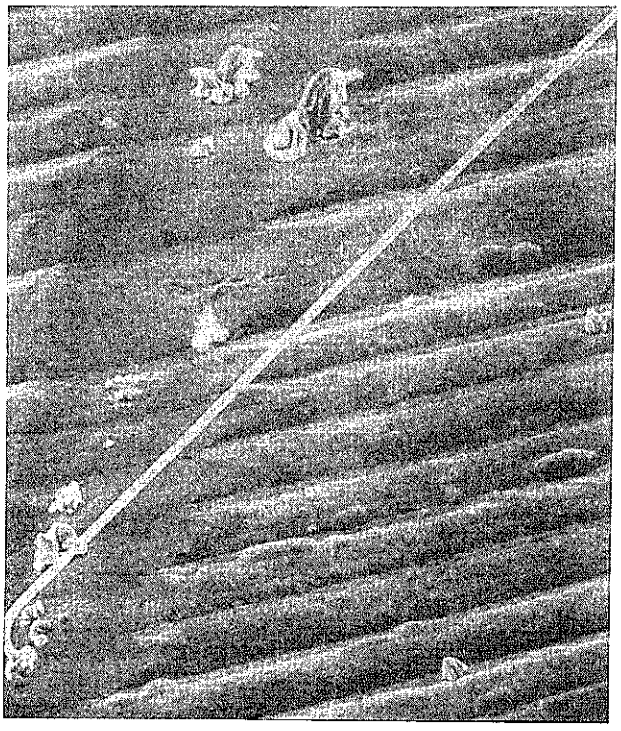

(c)

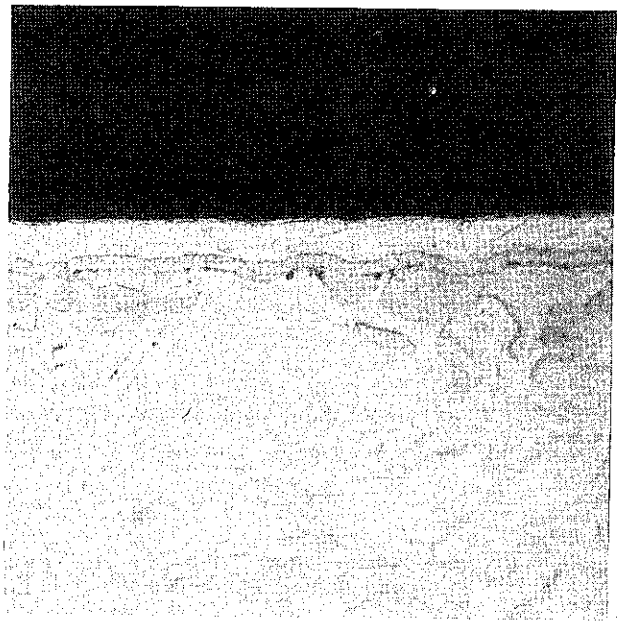

(d)

Specimen No. 10 at day 57 (a/b) and at day 181 (c/d) inspection

(a) Occasional short whiskers (×200)
(b) As (a) showing associated peaked nodules (×3000)
(c) Time period has increased growth length to 0.3 mm (×500)
(d) Microsection reveals copper barrier layer beneath tin (×600)

Figure 7. Normal tin-plating with copper barrier layer on brass.

(i)

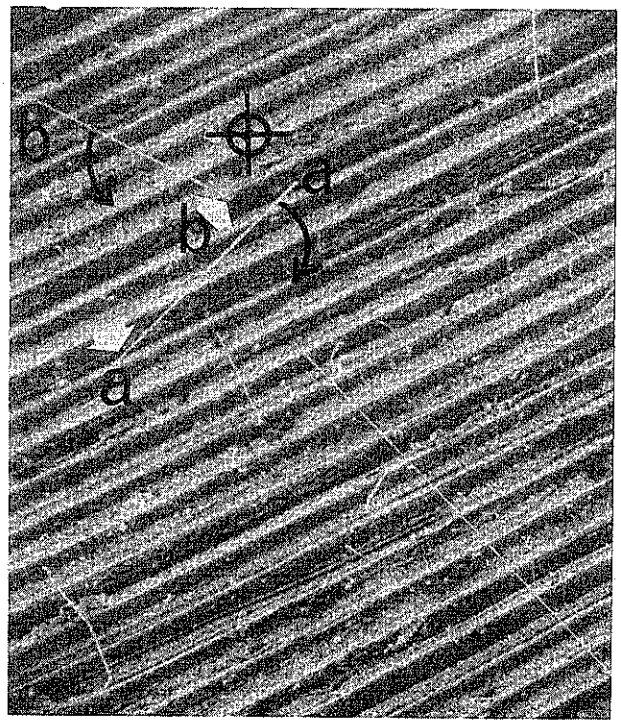

(iii)

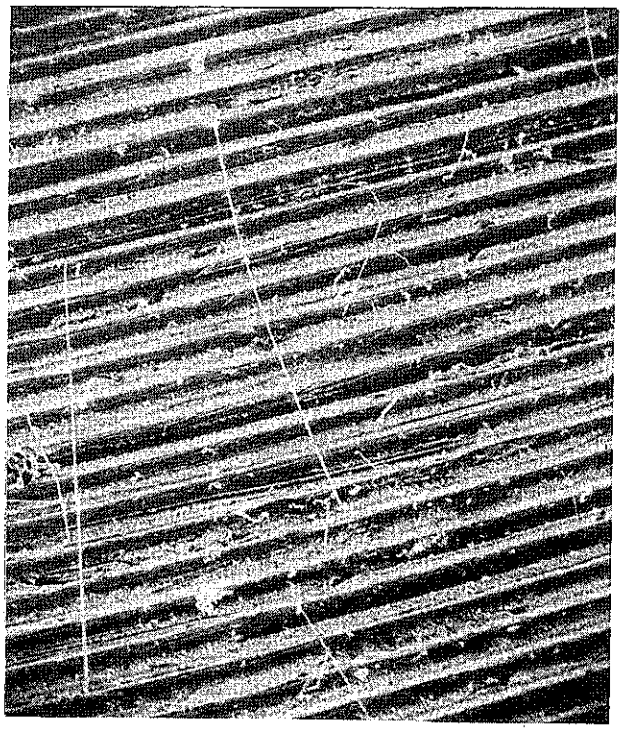

(ii)

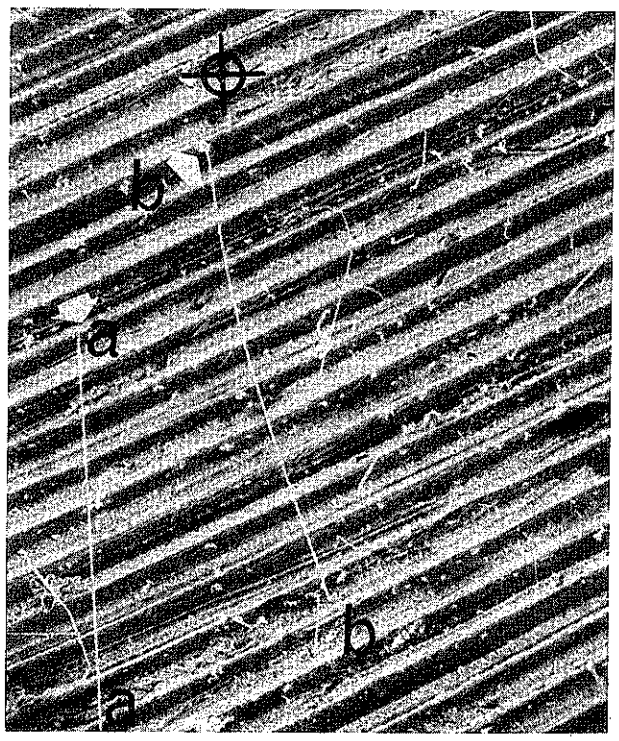

Specimen No. 13 at day 57 (i), day 181 (ii) and day 634 (iii) inspections (i, ii and iii all ×200).

Identical surface area:

- Attention is drawn to the whiskers 'a' and 'b'. The white arrows show where they emerge from the tin surface.
- Despite the fact that they contain no kinks, their growth orientation has changed, causing both whiskers to sweep through about 140° (compare (i) with (ii)).
- During this 124-day period, whiskers have grown as follows:

increase in length	Rate of growth
'a' — 125 μm	ca. 1μm/day
'b' — 110 μm	ca. 1μm/day

- The whiskers 'a' and 'b' have not altered their position or length during the period between the day 181 and day 634 inspections.

(iv)

(v)

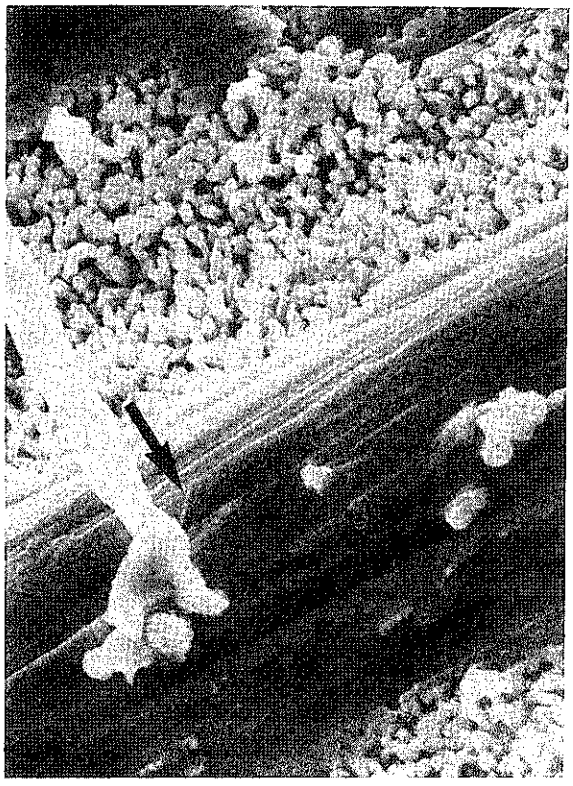

(vi)

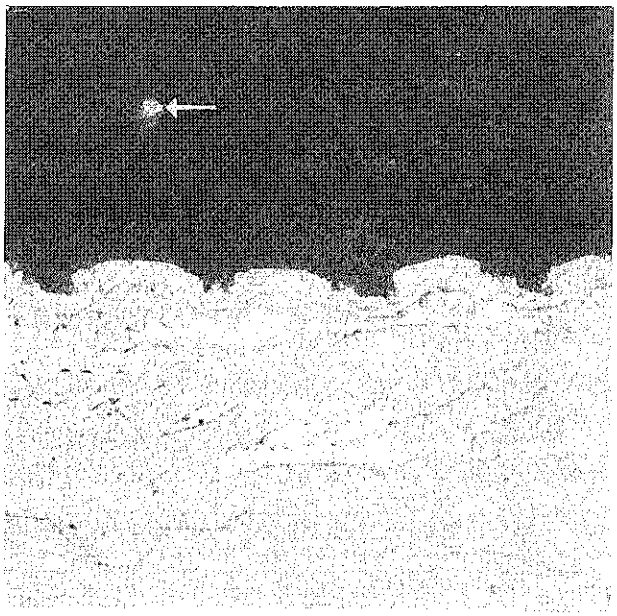

(iv) Detail of whisker having length of 700 μm. Changes in growth direction has caused it to become ensnarled with other whiskers. Relatively large latent energy is contained within this bowed volume (×200).

(v) It is remarkable that such long whiskers (i.e. that shown in (iv)) produce no evidence of surface subsidence. The arrow details the smallest whisker ever documented, which has a diameter of 6 nm (×3000).

(vi) Microsection reveals sectioned whisker and abnormal tin thickness (×600).

Figure 8. Abnormal tin plating on brass with copper barrier layer.

(a)

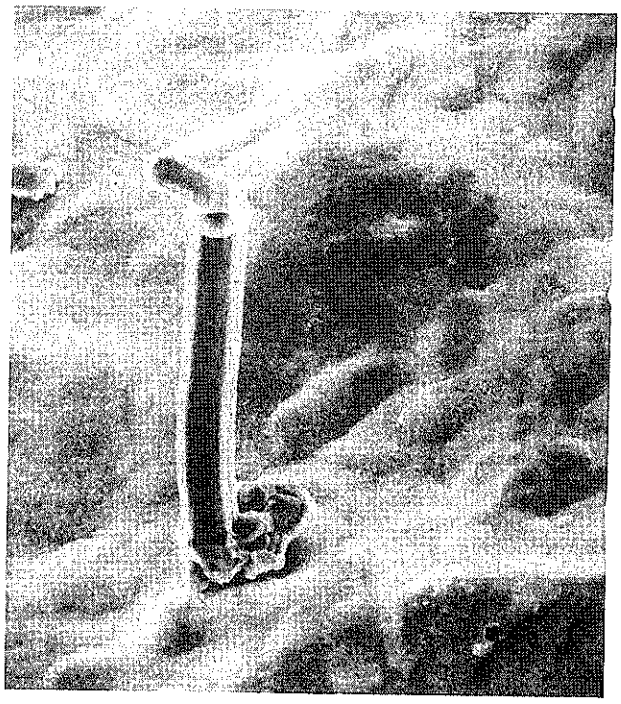

(c)

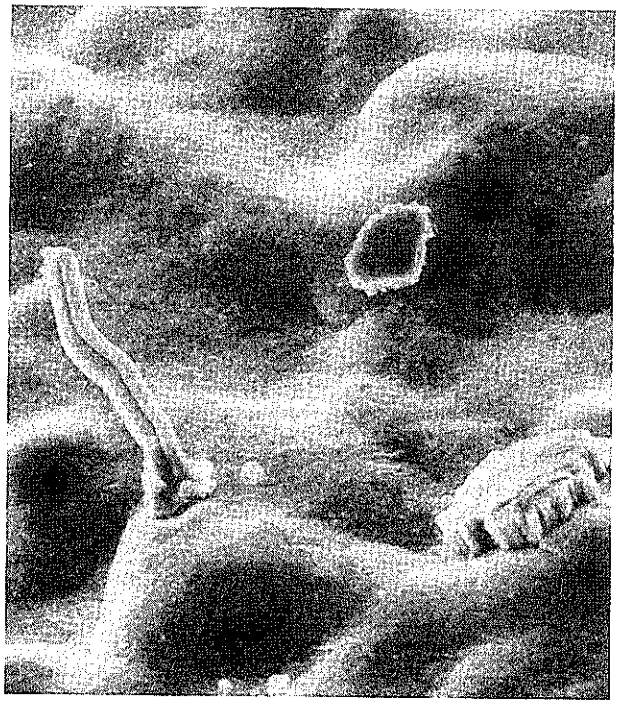

(b)

(d)

Specimen No. 16 at day 57 (a), day 181 (b) and day 634 (c and d) inspections

(a) Apparently the initiation of blocky columnar growths (×1000)
(b) Short whisker has grown, but blocky shapes remain virtually unaltered (×1000)
(c) No morphological change at day 634 inspection (×1000)
(d) Microsection through block reveals no associated surface subsidence (×600)

Figure 9. Organically contaminated tin-plating on copper barrier layer.

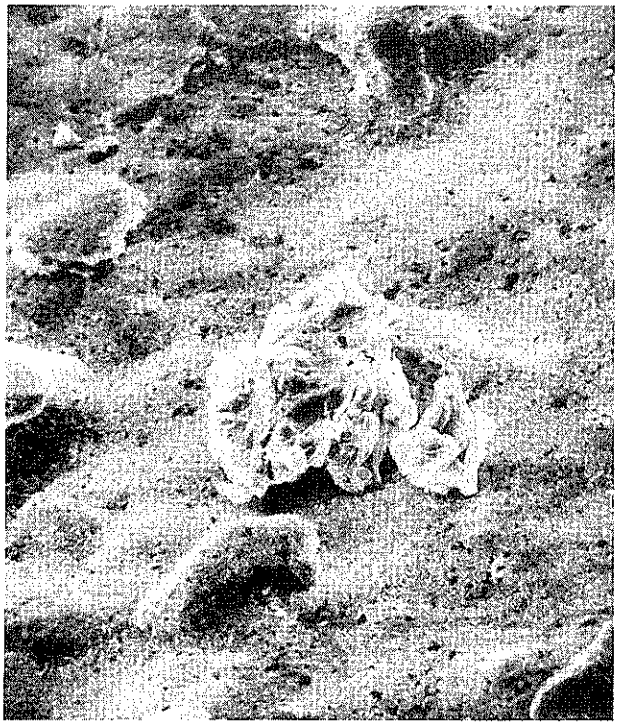

Specimen No. 19 at day 634 inspection

The first indication of a nodular growth identified after 634 days of storage. The dark inclusions appearing on the fused tin coating were picked up from the sand-bath oven. These dark speckles also exist on the nodule confirming it to be a growth rather than an extraneous particle.

Figure 10. Fused tin coating on brass C-ring (no copper barrier layer).

(a)

(b)

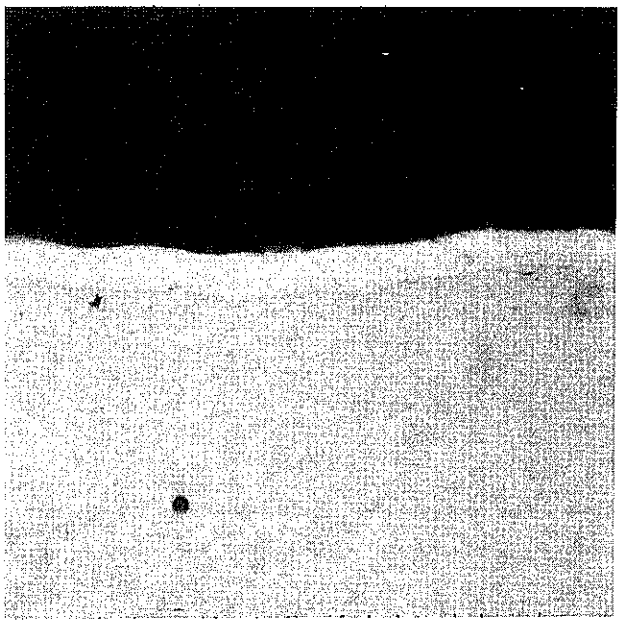

Figure 11. Tin-plated steel after 181 days (Specimen No. 21). Short stubby needles are only occasionally observed (a, ×1000) on this otherwise featureless surface (b, microsection, ×600).

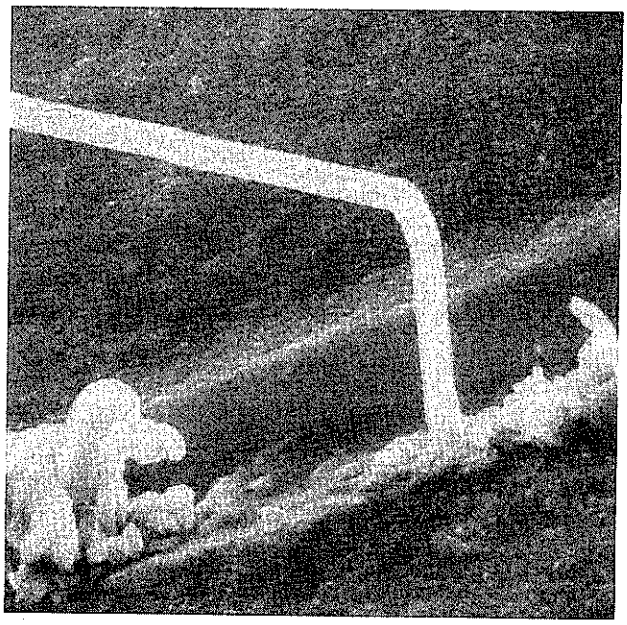

(a)

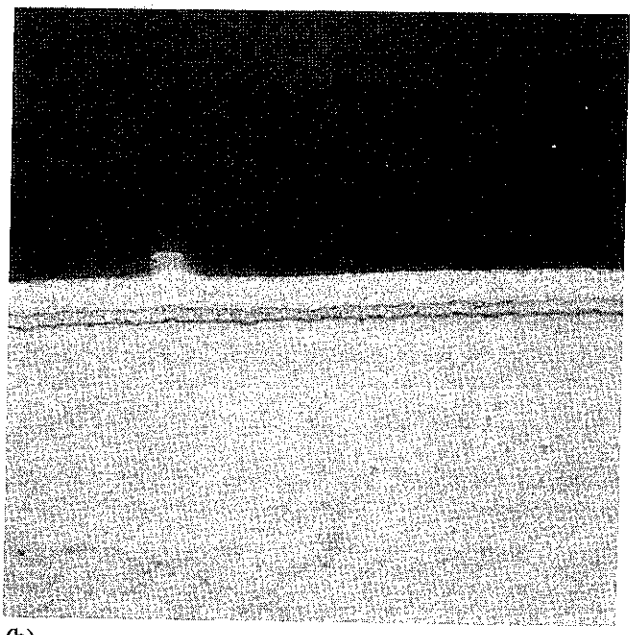

(b)

Figure 12. Tin-plating on steel copper barrier layer after 181 days. Specimen No. 30. Dense population of long whiskers (a, ×1000) emerge from this nodule-supporting surface (b, microsection, ×600).

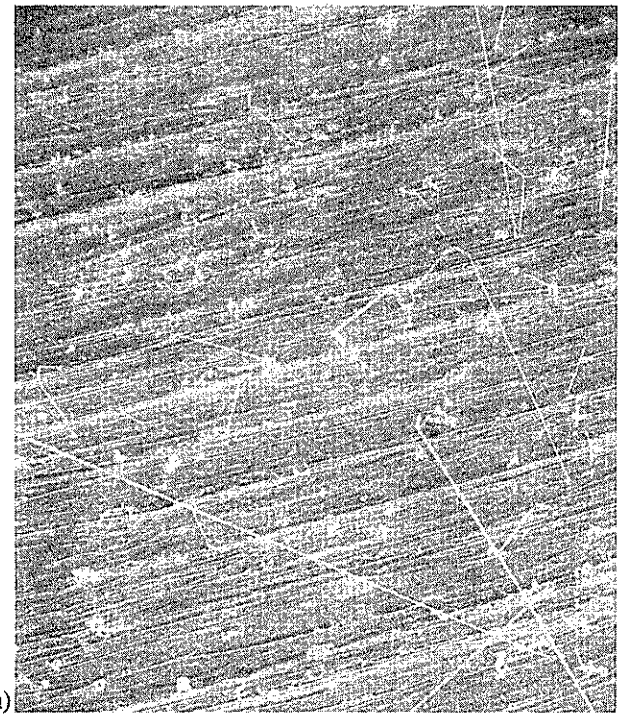

(a)

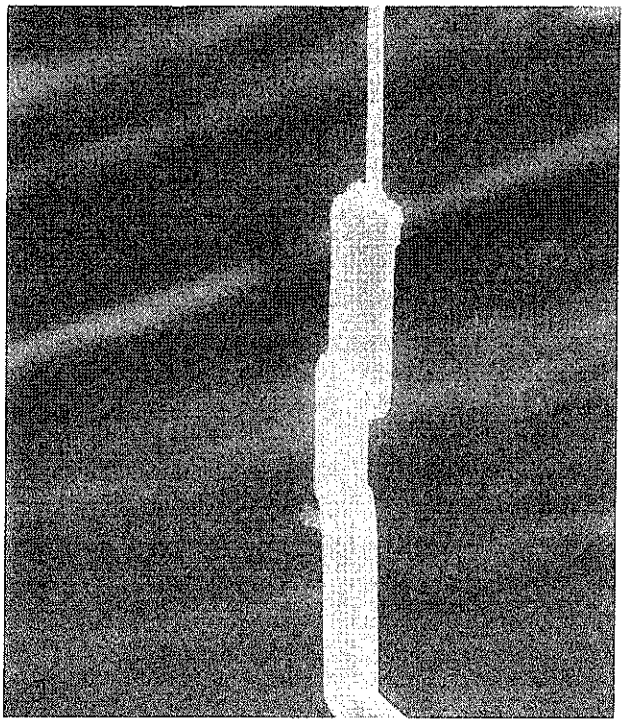

(c)

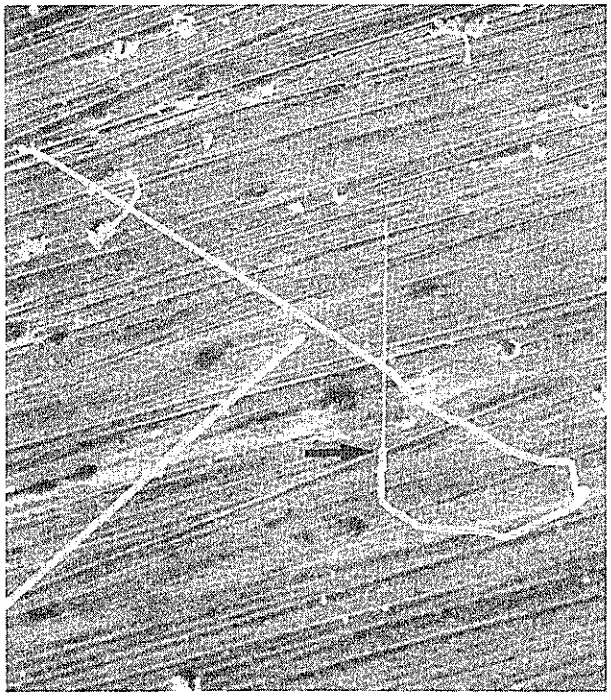

(b)

Specimen No. 35 at day 57 (a) and day 181 (b and c) inspections.

(a) Prolific whisker growths (×200)
(b) An unusual whisker exhibiting many changes in growth direction (×300)
(c) Detail of whisker shaft arrowed in (b); note steps and dramatic change in cross-sectional diameter (from 0.6 to 2.8 μm)(×3000).

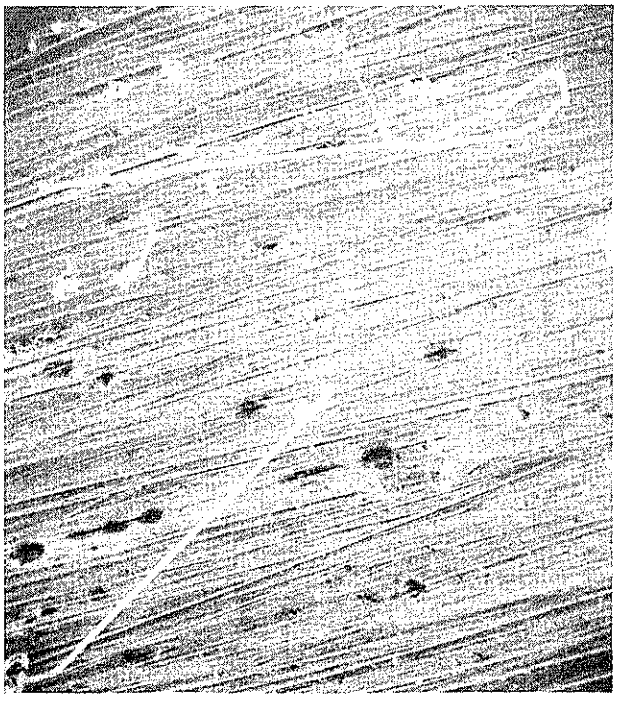

(d)

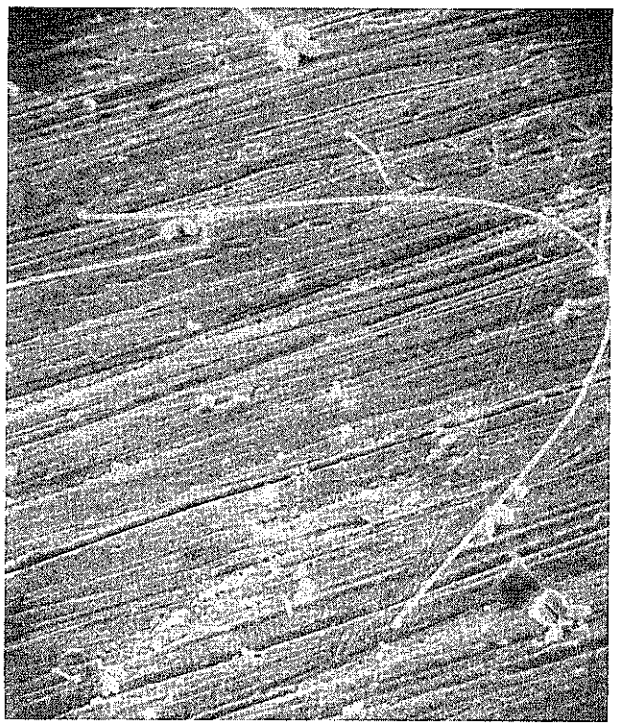

(e)

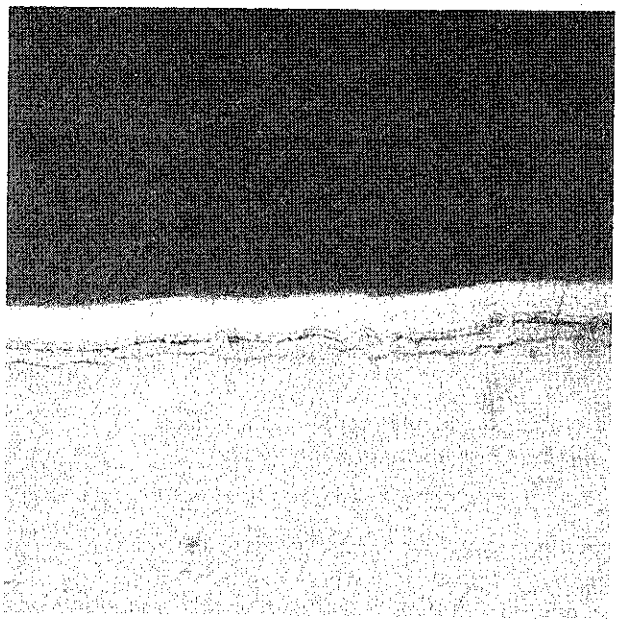

(f)

Specimen No. 35 at day 634 inspection

(d) Same area as (b) showing some rotation of 'unusual' whisker.
(e) Whiskers with low projection angles become pinned by other surface obstructions as they gyrate during growth (×800).
(f) Microsection showing copper barrier layer.

Figure 13. Abnormal tin-plating on steel with copper barrier layer.

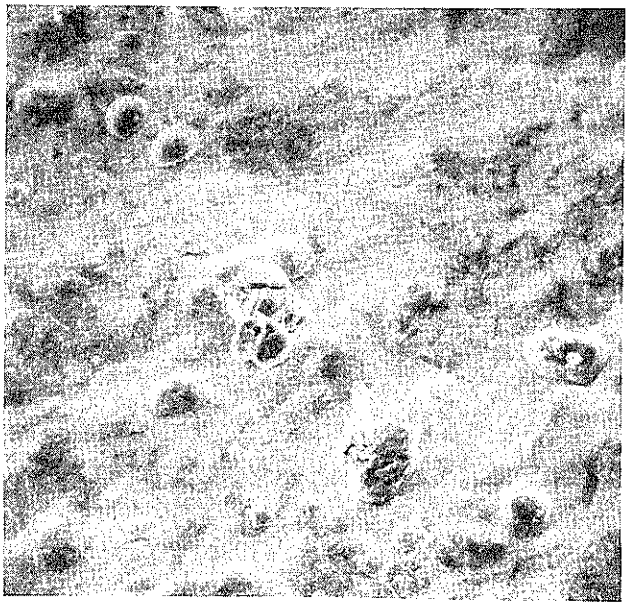

Specimen No. 38 at day 634 inspection

Tin surface supports the same blocky columnar protuberences and short whisker growths as those seen in Fig. 9 for the same finish on a brass substrate (×500).

Figure 14. Organically contaminated tin plating on steel C-ring with copper barrier layer.

× 2000

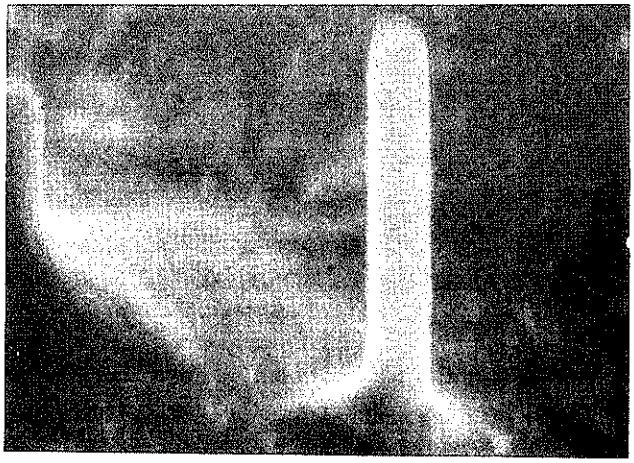

×10 000

Specimen No. 40 at day 1269 inspection.

Figure 15. Fused tin on steel with copper barrier layer.

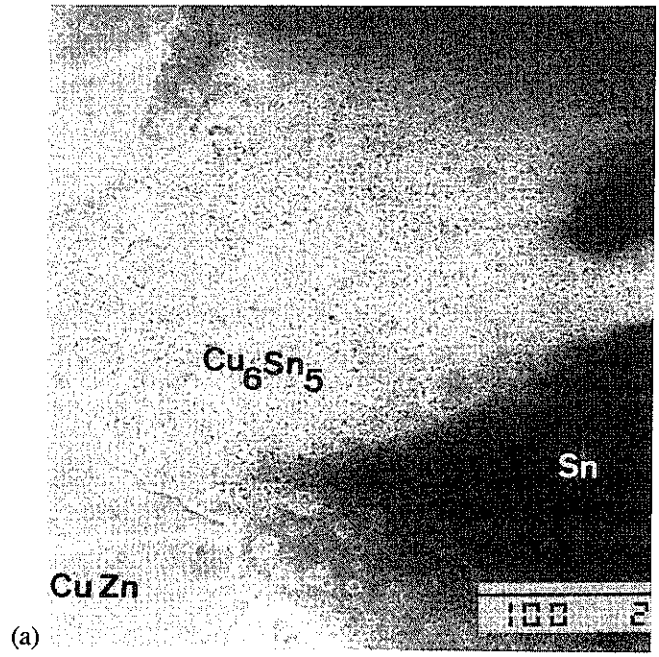

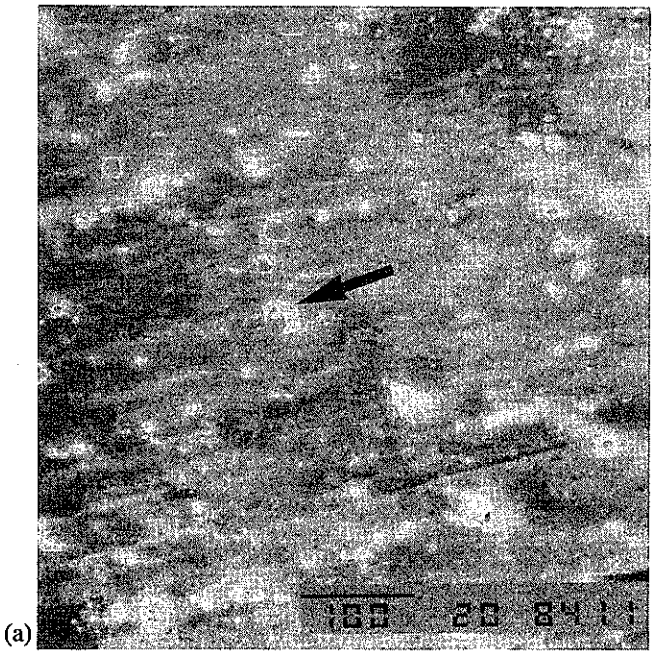

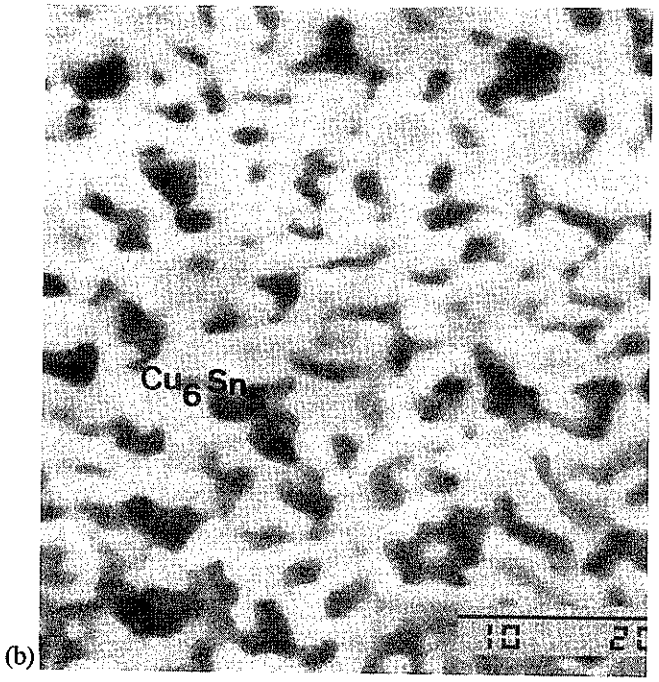

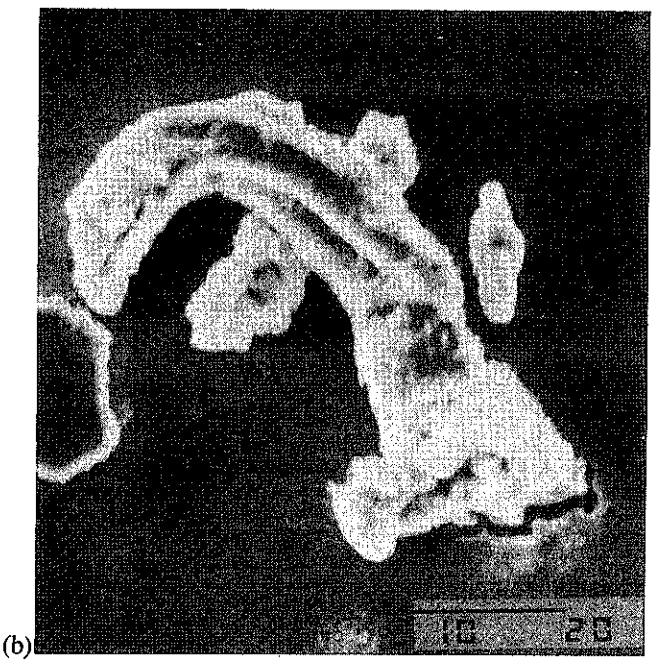

Figure 16. Cathodically stripped tin from surface of brass C-ring after 634 days of room-temperature storage. Specimen No. 7 previously finished with 'contaminated' tin-plate. Differential stripping rates have revealed three separate layers in (a): remaining tin, intermetallic, and the brass substrate. The intermetallic is irregular, as detailed in (b).

Figure 17. Surface of Specimen No. 16 (contaminated tin-on-copper-on-brass) after cathodically stripping most of tin-plating. One whisker is arrowed on (a) and detail in (b). The surface supports a residue of the flour particles. The whisker has a length of 50 μm and is surrounded by a flat, continuous layer of intermetallic compound.

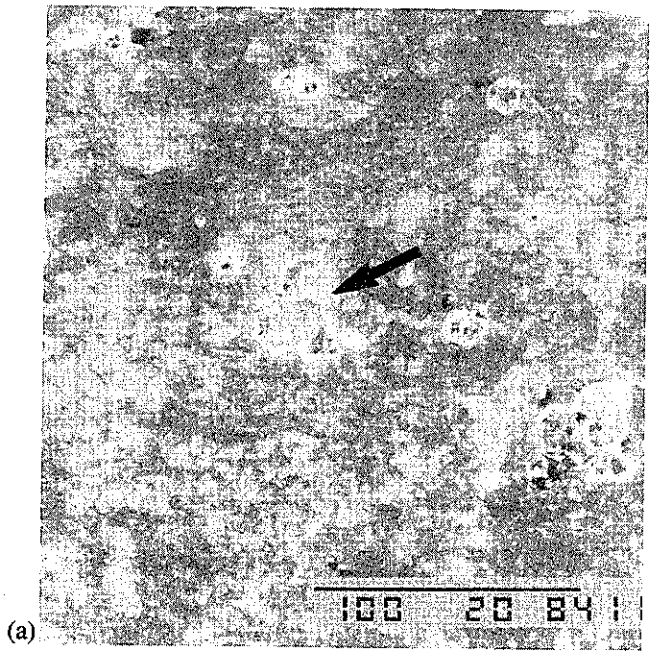

Figure 18. Surface of Specimen No. 36 (contaminated tin-on-copper-on-steel) after cathodically stripping most of tin-plating. Several nodules were observed (a), but no whiskers. (b) details a nodule supported on layer of intermetallic and surrounded by organic contaminant.

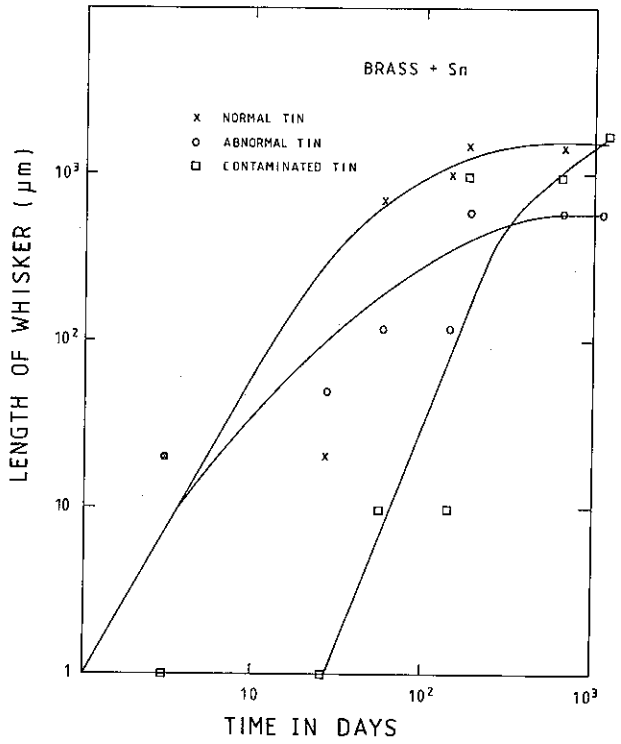

Figure 19. Logarithmic plots of maximum growth (μm) against time (days) for tin-plated brass specimens.

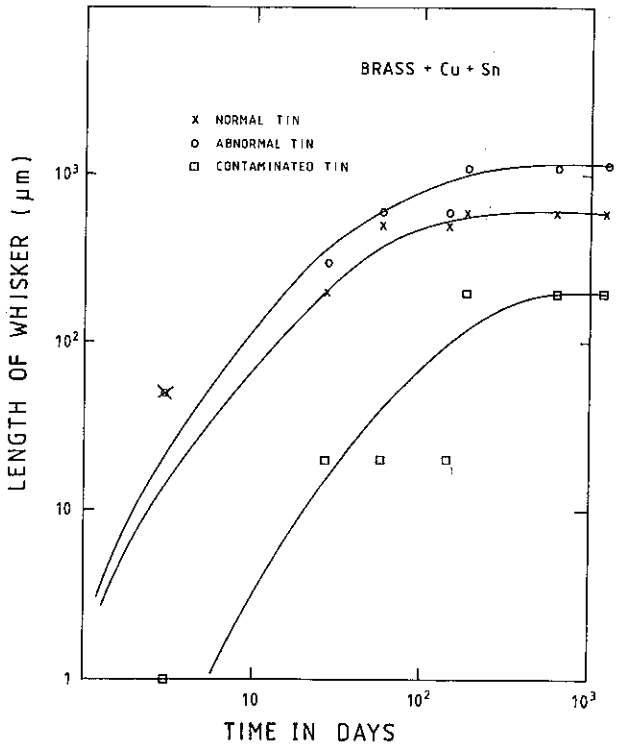

Figure 20. Logarithmic plots of maximum growth (μm) against time (days) for tin-on-copper-on-brass specimens.

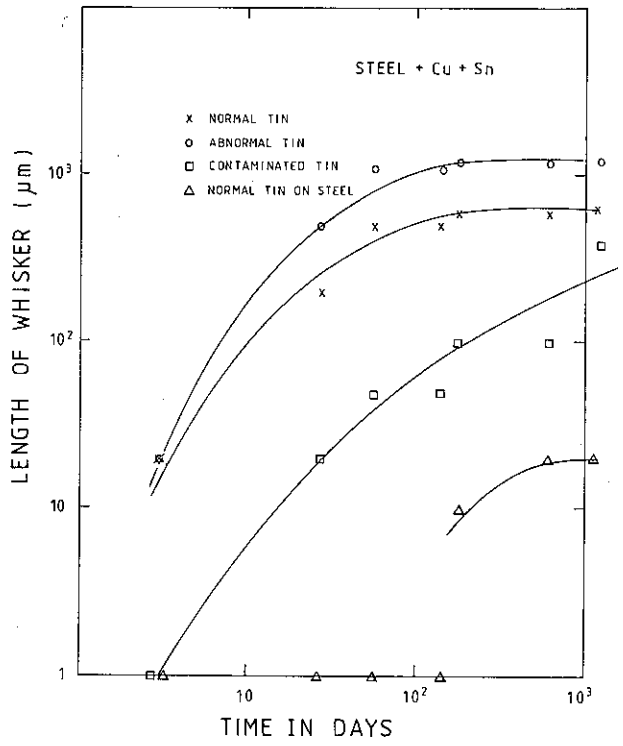

Figure 21. Logarithmic plots of maximum growth (μm) against time (days) for tin-plated steel, with and without a copper intermediate layer.

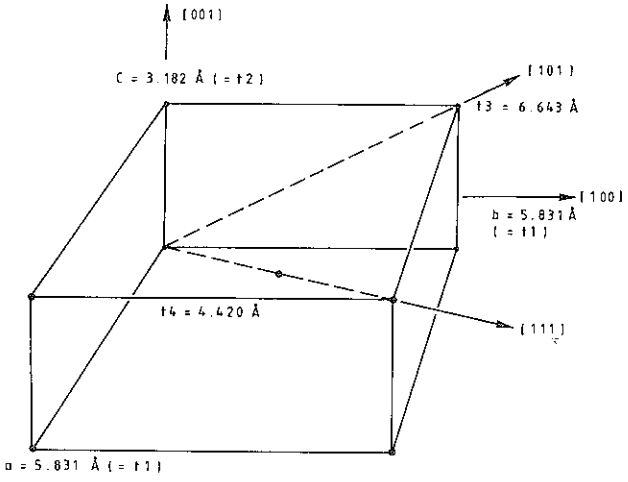

Figure 22. Illustration of the tetragonal crystal structure of white tin with identified unit cell parameters and possible growth directions. (Basic data from Swanson, H.C., & Tage, E., *'Crystallographic Structures'*. Nat. Bur. Standards Circular No. 539, **1**, 25 (1953)).

CALCULATION FOR FIGURE 23

Demonstration of calculating unit-cell parameter and indexing

Constants: Radius of camera, R = 28.65 mm
Wavelength of CuK alpha, λ = 1.5415

Average sin μ = 0.232

$t \sin \mu = n\lambda$

$$t = \frac{n\lambda}{\sin \mu} = \frac{1.5415}{0.232} = 6.64 \text{ Å}$$

for central layer line, θ = Bragg angle

θ = 16.0
= 22.5
= 36.8
= 57.5

$$d = \frac{\lambda}{2 \sin \theta} = 1.287 \text{ Å}$$

Miller Index of spacing, hkl = $41\bar{1}$

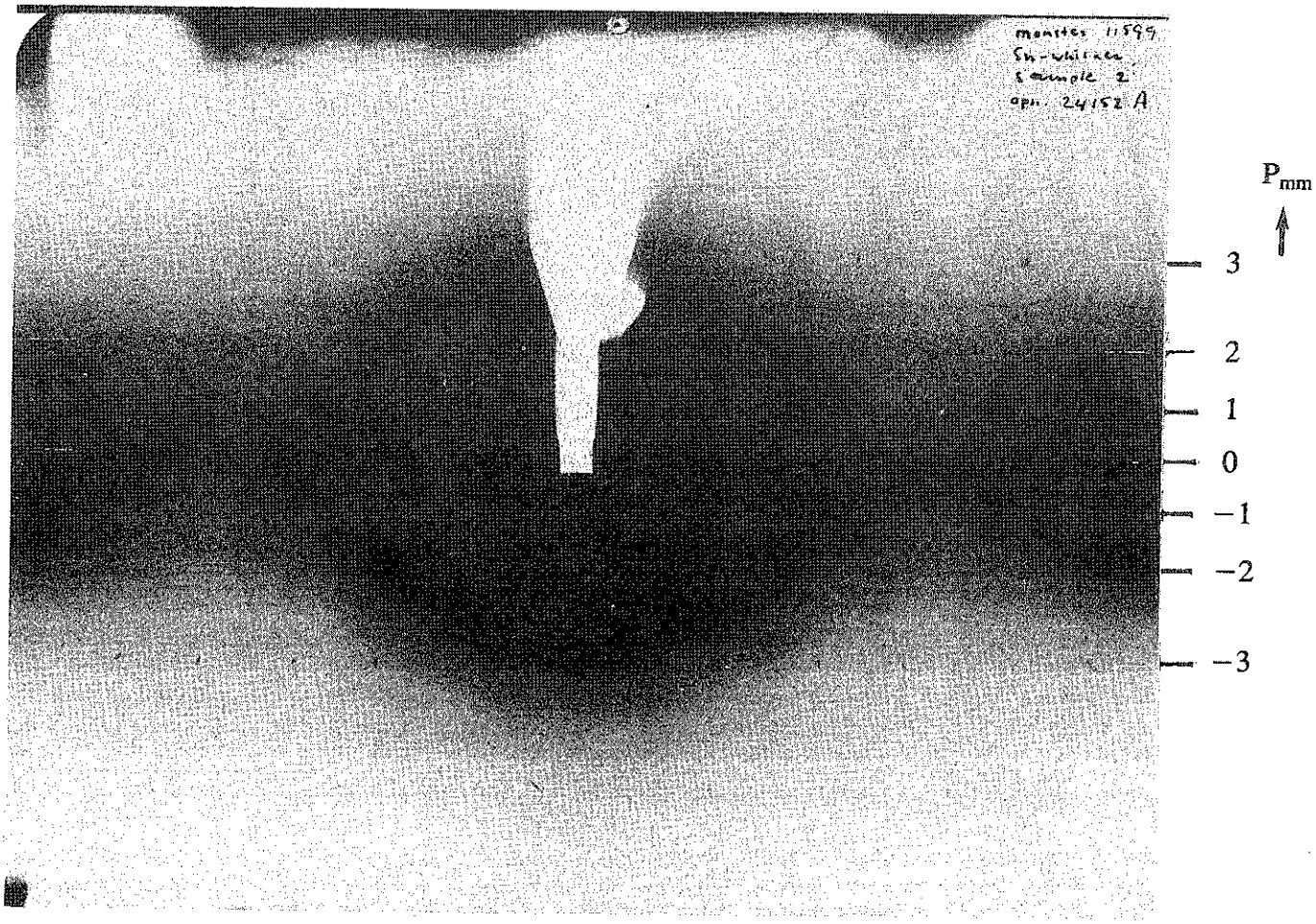

Figure 23. Diffraction photograph of tin whisker Sample 2.

From photograph:

LAYER-LINE	MEASUREMENT OF LAYERS FROM CENTRAL LAYER (WHITE SCRATCH) (IN MILLIMETRES)			$\tan \mu = \frac{P}{R}$	$\sin \mu$
	LEFT	RIGHT	AVERAGE (P)		
1	7.0	6.9	6.95		
				(6.92)	0.2415	0.235
−1	6.9	6.9	6.90		
2	14.8	15.0	14.90		
				(14.97)	0.5225	0.463
−2	15.0	15.1	15.05		
3	27.4	28.0	27.70		
				(27.60)	0.9634	0.694
−3	27.4	27.1	27.55		

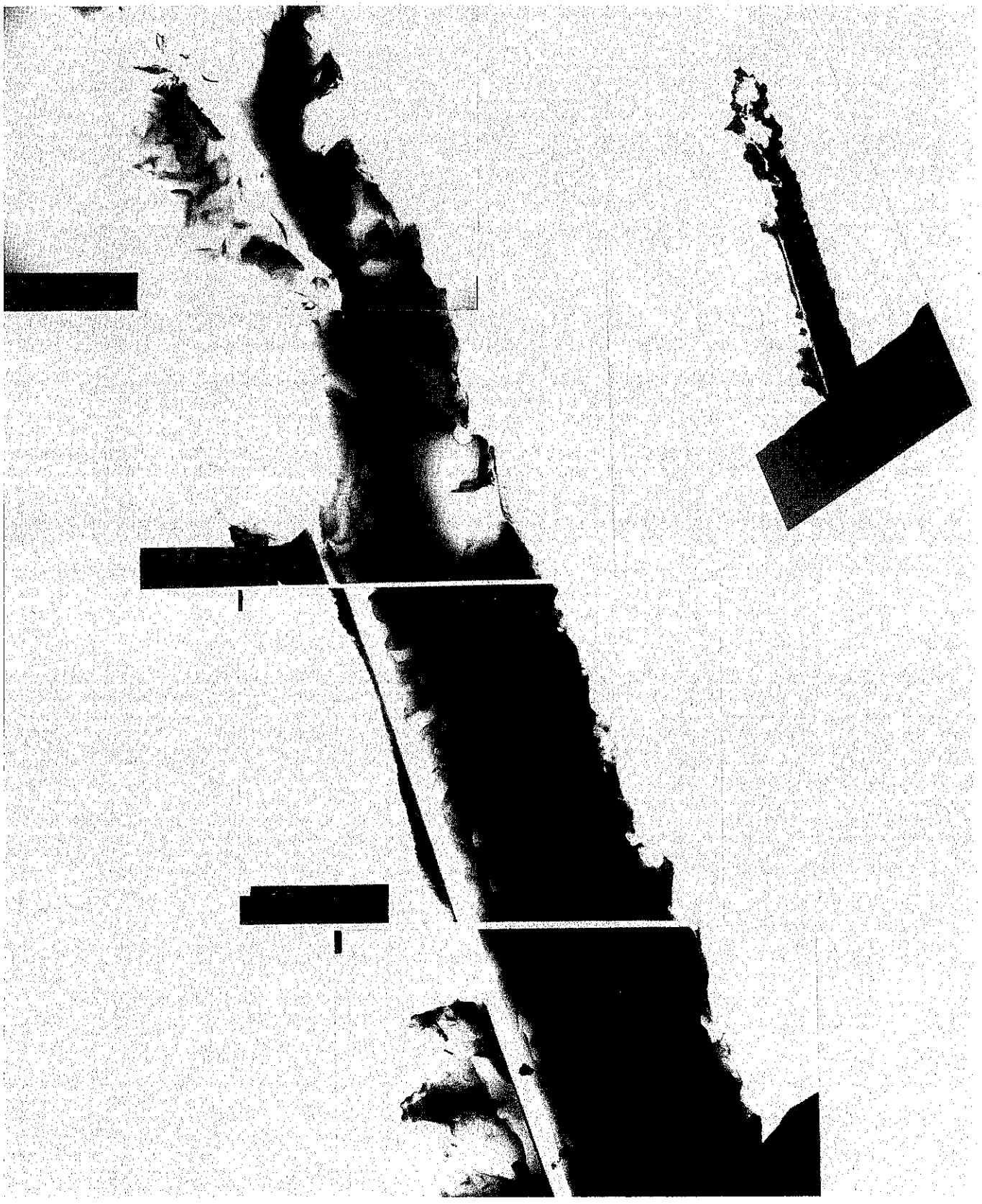

Figure 24. Composite bright field image of thin whisker prepared into a wedge-shape. This tin 'slice' appears to have passed through a flute on the whisker's shaft.

4. DISCUSSION

4.1 TIN SURFACES

Tin probably owes its wide use to two main properties: it has a very good solderability and is non-toxic. It also has a low melting point (232°C) and can be passivated, but it is also relatively expensive compared with other protective metals such as zinc and cadmium. Tin can be plated from a number of commercially available baths. These are based on either acid-sulphate, alkaline-stannate or halogenated-tin electrolytes. The most common bath for the finishing of commercial electronics, a stannous-sulphate electrolyte, was utilised in our study.

The *mechanism of tin deposition* during electroplating onto a clean surface is complex and depends on the polarisation characteristic of the electrolyte immediately adjacent to that surface, and on the availability of different forms of lattice sites. Large energies will be needed to discharge a tin ion onto a free flat surface, whereas the most favourable practicable site would be a ledge on the lattice surface. When the growing ledge is the fault step of a screw dislocation, the plating will grow in thickness as the spiral winds itself up [11]. It is thought probable that when the current density is increased, the rate of ion arrival at the surface is so great that there is insufficient time for the spiral to operate. Instead, fresh sites are generated and many ledges can be nucleated for further growth. These generate a fine, polycrystalline microstructure within the plating. Dendritic outgrowths (or 'treeing') are created at very high current densities, when there is a tendency for preferential outward growth from the nuclei, rather than a lateral planar growth.

The *metallurgical results* of this study show that each of the C-ring specimens has been plated with a matt, not-so-bright smooth tin deposit that is considered to be composed of a fine-grained microstructure of high chemical purity. Similar topographies were noted for each of the three plating bath conditions and were also identical for the various surface materials (brass, copper and steel). The macroscopic surface variations that replicate the machine markings seen on the C-ring will not be considered as a variant. The 'normal' and 'contaminated' platings were noted by sectioning to have slightly greater thicknesses than the 'abnormal' tin-plate and this is probably due to the far lower tin content of the 'abnormal', high-current-density bath, as recorded in Table 1. The commercial brighteners were added in the same concentrations to each of the bath types and are therefore not considered to constitute a variant.

The metallurgical characteristics of tin-plated layers will now be considered with reference to the tin finishes that were applied to the C-ring experiments. Some fundamental behaviours and theories related to solid metals will be summarised as groundwork to the discussion of tin-whisker growth mechanisms presented in the following section.

The tin-plated layer can be considered to be attached to the brass, steel or copper substrate by means of metallic bonding. It is also convenient to consider the semi-empirical rules that result from Hume-Rothery's studies of solid solubility when we consider the possibility of alloying between the substrate and tin-plating by solid-state diffusion. These rules refer to the difference between the relative atomic radii of the participating elements. If the difference between atomic sizes exceeds about 14–15%, solid solubility is restricted.

Additional rules related to electrochemical differences and their relative valancies will establish whether intermediate phases will occur.

The atomic diameters [12] of each C-ring material constituent are recorded below and compared with that of the tin atom:

Tin	0.280 nm	
Copper	0.255 nm	8.9% atomic size difference
Zinc	0.266 nm	5.0% atomic size difference
Iron	0.252 nm	10.0% atomic size difference.

Each element is noted to have a favourable size factor (deviating less than 15% from that of tin) so that, under certain conditions, one can expect solid-state diffusion of the substrate atoms into the crystal lattice of tin and the formation of a substitutional alloy.

It will be recalled that the electroplated tin structure layer will consist of defects such as screw dislocations, and a large grain boundary network when the layer has a small grain size. Other defects will include vacancies and stacking faults.

The treatment of electro-deposition given by Gabe [11] clearly shows the discharge of metal ions to be a rate-controlled process that is dependent on characteristics such as polarisation. Under some plating conditions, the orientation of the base metal is

copied by the deposit, particularly if the base-metal grains are freshly etched and the plating system employs small current densities and electrolytes without colloidal additions. On the surface, there is a variety of lattice sites, each having its own order of free energy. Clearly a lattice vacancy has a minimum energy, and the largest energy is required to deposit an ion onto a free flat surface. The figures included in the work of Gabe [11] clearly show that ledge sites, particularly those around a screw or ledge dislocation, are the most practical sites for metal ion deposition. The continual nucleation of fresh layers is not observed when emerging screw dislocations are present on the substrate surface and *growth is by the winding up of the spiralling dislocation.*

The electro-deposit has also been described by Barrett [13] who, following work into the nature of the deposit's orientation by X-ray and electron diffraction, found that the plated material is likely to assume its own texture such that the crystal axes stand perpendicular to the substrate (i.e. parallel to the direction of current flow). The texture of electro-deposited tin was found to be in both the [111] and [001] directions.

The number of dislocations in an as-plated tin layer is likely to be high, particularly as these electro-deposits can have internal stresses as great as $10-20$ kg/mm^2. The presence of a high dislocation concentration together with a large, usually compressive, internal strain within a tin-plating establishes an unstable microstructure with local sites of high energy content [11]. Any additional strain energy can produce a change or *recrystallisation* within the plated layer; this lowers the total free energy of the plated layer, according to the laws of thermodynamics.

When recrystallisation takes place in this layer, as a result of a combination of increased strain and/or temperature, the dislocation concentration drops back to a lower level. The increased strain may result from such factors as mechanical loading (e.g. during the clamping of the C-ring specimens) or the growth of an intermediate phase that with a lower density and a consequently larger volume causes internal strains. Another source of increased strain energy can result from diffusion effects (due either to volume diffusion by vacancy and atom interchange mechanisms, or to grain-boundary diffusion when the pronounced imperfections in grain boundaries will sustain faster diffusion than within the grain proper). The diffusing components may have different diffusion coefficients, resulting in a net transport of material across the plane that originally separated the plating from the substrate. (This is called the 'Kirkendall effect' which can be shown experimentally between metals such as gold and aluminium.) The internal oxidation of metals can also account for an increase in strain energy.

The recrystallisation process is the equivalent of annealing in accommodating some of the disregistry produced in the crystal lattice as a result of introducing such high concentrations of dislocations. The atoms will tend to rearrange themselves so as to achieve a minimum energy state by eliminating vacancies and dislocations.

Recrystallisation of a metal such as tin (in its pure state) can occur at relatively low temperatures, as shown in Table 11. This table shows that very high purity copper (99.999%) recrystallises at a temperature as low as 120°C and pure aluminium has a recrystallisation temperature of only 80°C. However, by increasing the impurity level there can be up to a three-fold increase in recrystallisation temperature. Table 11 shows the recrystallisation temperatures of pure tin and zinc to be below room temperature, at −4°C.

TABLE 11. *Approximate recrystallisation temperatures for several metals and alloys**

MATERIAL	RECRYSTALLISATION TEMPERATURE, °C
Copper (99.999%)	120
Copper, 5% zinc	315
Copper, 5% aluminum	288
Copper, 2% beryllium	370
Aluminum (99.999%)	80
Aluminum (99.0%+)	288
Aluminum alloys	315
Nickel (99.99%)	370
Monel metal	590
Iron (electrolytic)	400
Low-carbon steel	538
Magnesium (99.99%)	66
Magnesium alloys	230
Zinc	10
Tin	−4
Lead	−4

* Taken from Guy [4]

At the onset of the C-ring experiment, the tin-plated surface is composed of pure tin (even the contaminated bath produces a pure tin finish with occluded particles of flour). The experimental results (Figs. 16–18) clearly show that, as the shelf time increased, the intermetallic compound Cu_6Sn_5 was initiated and grew in thickness at both the tin-to-copper and the tin-to-brass interfaces (irregularly at the latter).

The surface analyses (Table 9) also show that, even at room temperature, appreciable amounts of zinc (and to a far lesser extent copper) have diffused from the brass substrate to the tin surface during the course of the experiment. Zinc and copper are also present in the nodules that quickly appeared on those C-ring samples machined from brass.

The author has reported [15] on the rapid diffusion of zinc through tin platings to form thick non-solderable zinc-oxide layers on brass-substrate terminal pins. The mechanism for segregation or alloying of metals like zinc onto a tin surface is not exactly known. Two hypotheses are suggested. One considers the lattice strain energy. The zinc atom is smaller than the tin-solvent atom and therefore produces a lattice strain. Since that lattice strain brings about a higher energy state in the tin lattice, the plating tends to reduce its energy level. This is achieved by squeezing out the zinc solute where it segregates onto the tin surface.

The second hypothesis considers the concept of surface energy. The very pure, as-plated tin surface can be considered to be in a highly energetic state. Diffusion and segregation of zinc to this surface reduces the surface energy.

The foregoing accounts, related to tin *recrystallisation* and the *diffusion* of substitutional elements such as copper and zinc through tin-plating, have not taken into account the effects of temperature or time. Certainly, higher temperatures will increase the rates of those changes in microstructure; this aspect will not be considered here as most case studies and the C-ring experiments relate to tin-plating held at a constant temperature (room temperature). Only time will be treated here as a variable.

No references have been found to room-temperature isothermal recrystallisation curves for tin. The usual method for producing such a curve is to place many samples of a fine-grain tin-plated material in the same environment (and same temperature) for a very long period. Specimens are removed periodically, and their percentages of recrystallisation are determined by microscope examination. Such methods generally yield isothermal recrystallisation curves of the type shown in Figure 25 (from Ref. 14). It is assumed that such a curve exists for tin and can be considered to account for the recrystallisation of tin-plate stored at room temperature. Initially, the residual stresses in the tin plate are removed (*stress-relief*) and after a nucleation period high-angle grain boundaries pass through the material causing the small grains to grow to an equi-axed, stress-free and low-defect state (*recrystallised condition*). After this, cannibalism might occur among the new population of grains (termed *grain-growth*). Usually, all boundaries migrate at roughly equal rates to produce grains of equal sizes. Occasionally, migration can be limited to only a minority of boundaries, so that only a few grains grow at the expense of the rest. This is called *exaggerated grain growth.*

Recrystallisation rates for tin are not known for samples held at room temperature, although isothermal recrystallisation curves have been studied at 150°C, 170°C and 180°C by French researchers [16]. That work evaluated the migration of deformed grains by direct microscopic observations. Although the progress of each migrating grain boundary was noted to be uniform, the growth rate was dependent on the crystallographic orientation of the grain and the growth direction. Typical migration rates were 3, 30 and 640 μm/s at 150, 170 and 180°C, respectively. One value for the speed of migration was recorded in that

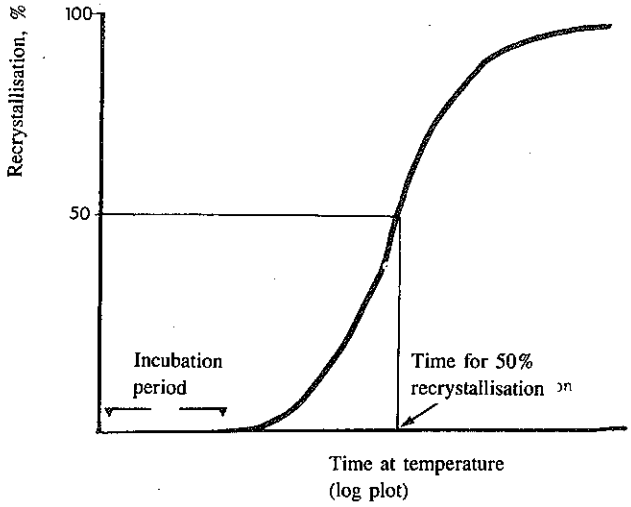

Figure 25. A typical isothermal recrystallisation curve (for constant temperature and alloy composition).

paper at a temperature of 100°C, this being 1 μm/s. It is evident that the extent of recrystallisation will be strongly dependent on both the temperature of storage and the amount of stored energy (e.g. the number and distribution of dislocations, stacking faults and other lattice imperfections that exist within the grains of tin).

A standard relation [16] between the rate of recrystallisation, V, and temperature (T), in degrees Kelvin is given by:

$$V = V_0 \exp\left[\frac{-Q}{RT}\right]$$

where the energy of activation Q, and V_0 are constants.

When the elevated temperature results from Reference 16 are considered, it can be expected that the rate of recrystallisation at room temperature will be approximately 1000-fold slower than at 100°C (i.e. 1 nm/s).

An important conclusion can be drawn from a detailed comparison between the *coefficients of diffusion* for the metals, such as tin, cadmium and zinc, that are known to be whisker-forming and those for alternative metals that are commonly electroplated, but have not been observed to initiate whisker growths. The diffusion coefficient, D, has been found [12] to be exponentially related to temperature by the Arrhenius-type expression:

$$D = A \exp\left[\frac{-Q}{RT}\right]$$

where

A = a constant that depends on the frequency of atom vibration of the diffusing atom (units are cm^2/s).
Q = activation energy, i.e. the energy required to make an atom jump from one equilibrium lattice position to another (units are kcal/mol or preferably in SI units, converted to joules/mol by multiplying by 4.185).
R = universal constant (1.987 cal/mol/K)
T = absolute temperature, K.

An extensive collation of data related to diffusion in metals is presented by Smithalls [9]. *Self-diffusion* of the whisker-growing electroplatings at room temperature (293 K) is exceedingly slow and coefficients must be extrapolated from the data [9] by means of the Arrhenius equation.

Several experimental values for A and Q have been determined from experiments that utilised thin layers of 99.998% tin and a radioactive tin diffusant [original references: Meakin et al., *Trans. Met. Soc., AIME,* 1960, **218**, 463, and Coston, *J. Phys. Chem.*, 1964, **68**, 2219]. The results gave conflicting values, particularly when self-diffusion was either parallel to or perpendicular to the c-axis of the tin lattice. Smoothing the reported values gives the following results (with tin at 178–222°C, A=7.0 cm^2/s and Q=104181 joules/mol/K):

$$D = 7.0 \exp \frac{-104181}{RT/K}$$

This relationship may be used to extrapolate an approximation of D at room temperature (293 K):

$$D_{(Sn,\ 293\ K)} = 1.8\times10^{-18}\ cm^2/s.$$

Similar values have been determined (from the data in Ref. 9) for the room-temperature diffusion coefficients of other whisker-forming elements:

$$D_{(Zn,\ 293\ K)} = 2.4\times10^{-18}\ cm^2/s$$
$$D_{(Cd,\ 293\ K)} = 1.0\times10^{-15}\ cm^2/s.$$

Predicted values for the room-temperature diffusion coefficients have also been calculated from the Arrhenius equation for non-whisker-forming metals. Typical results are:

$$D_{(Cu,\ 293\ K)} = 1.4\times10^{-37}\ cm^2/s$$

$$D_{(Au,\ 293\ K)} = 7.0\times10^{-33}\ cm^2/s$$

$$D_{(Ag,\ 293\ K)} = 7.5\times10^{-34}\ cm^2/s$$

$$D_{(Cr,\ 293\ K)} = 2.5\times10^{-75}\ cm^2/s$$

$$D_{(Pt,\ 293\ K)} = 6.2\times10^{-52}\ cm^2/s.$$

These calculations clearly demonstrate that the whisker-forming elements (tin, zinc and cadmium) possess room-temperature diffusion coefficients within

the range $10^{-15}-10^{-18}$ cm^2/s. Other commonly plated metals have exceedingly low room-temperature diffusion coefficients, within a range $10^{-33}-10^{-75}$ cm^2/s.

This striking difference is not coincidental and it must be presumed that the nucleation and growth of whiskers must depend on the plated material's ability to undergo solid-state diffusion easily; this will necessitate a low value of Q (i.e. a low activation energy to make an atom jump from one equilibrium position to another).

We shall now consider the influence of the C-ring substrate material on solid-state diffusion through the tin-plating, taking into account the diffusion coefficients of the elements zinc and copper. The Arrhenius equation will again be employed, together with data collated in Reference 18 from tracer-impurity diffusion experiments.

The diffusivity of zinc is greatest when parallel to the c-axis of pure tin crystals over the temperature range 135—223°C. The maximum diffusion coefficient can be expressed as

$$D_{(\text{Zn in Sn})} = 1.1\times10^{-2} \exp \frac{-124184}{RT/K}$$

Calculation for $D_{(\text{Zn in Sn})}$ at room temperature yields the value 1.2×10^{-11} cm^2/s.

Copper is most rapidly diffused parallel to the c-axis of tin grains and, according to Reference 9

$D_{(\text{Cu in Sn})}$ at room temperature is 2×10^{-6} cm^2/s.

The existance of an intermetallic layer (Cu_6Sn_5) at the phase boundary between copper or brass and tin results in an abrupt change in concentration and structure. It is important to remember that the diffusion equation discussed in this section is applicable to atom migration *within* a phase, so that the values of D, for either copper or zinc diffusion in tin, will be greatly modified as the intermetallic layer grows with time.

Zinc does not form an intermetallic compound with tin so that, although the Arrhenius equation indicates $D_{(\text{Zn in Sn})}$ to be theoretically less than $D_{(\text{Cu in Sn})}$, the presence of a Cu_6Sn_5 boundary layer is expected to retard the actual value for $D_{(\text{Cu in Sn})}$.

The surface analyses presented in the summary Table 9 show that zinc will rapidly diffuse through the tin layer and reach the C-ring surface. The presence of a copper barrier layer will act as a partially effective diffusion barrier, and copper itself will also tend to diffuse through the tin finish. A concentration curve based on these findings has been postulated for the interdiffusion of copper and zinc with tin (Fig. 26).

The microstructural imperfections contained in those tin-plated C-rings that were heated to slightly beyond the melting point of tin, and then slowly cooled to room temperature, will now be briefly considered. The few seconds during which the tin existed in a molten state has enhanced the diffusion of zinc from the brass substrate into the tin volume (see Table 9, specimen no. 19). The effectiveness of the copper barrier layer on specimen 20 is also demonstrated by the relatively low amount of zinc occurring on this specimen surface. The melting operation will have caused a double reaction layer of intermetallics between copper and tin to form at the original plating interface (Cu_3Sn and Cu_6Sn_5 form at elevated temperatures). The composition of the tin coating on specimen 39 (steel C-ring) remains pure and unchanged, indicating the low solubility of iron in liquid tin. However, copper from the copper intermediate layer on specimen 40 has diffused to the tin surface.

Cooling conditions from the tin solidification temperature will affect nucleation events and determine the final tin grain size, shape and, in the case of the brass C-rings, their compositional heterogeneity. The slow cooling rate is expected to result in the elimination of thermal stresses built into the coating and the existance of a very low dislocation substructure. It is thought that those dislocations that do form as a result of thermal stresses (differential contraction rates between the tin and its substrate) will be removed to the surface by a climb mechanism, or be mutually annihilated. In addition to being relatively strain-free, the fused tin grains will be large in comparison with the coating thickness. A final observation that is expected to throw much light on the whisker-growth mechanism is the fact that melting the tin layer will totally remove the screw dislocations that had previously existed either within, or emerging from the electroplated tin.

4.2 SPONTANEOUS TIN-WHISKER GROWTH

It is possible, in principle, to classify whiskers into two categories which differ primarily in terms of their growth mechanisms. The first category includes whiskers that crystallise onto a substrate from the vapour phase, the liquid phase or the solid phase, with *growth occurring at the tip.*

The second category contains whiskers that have grown spontaneously from the solid phase with *growth occurring at the base of the whisker.* This category appears to contain only pure metals, most commonly tin, cadmium and zinc. They grow at room temperature and growth rates have been accelerated by the application of high pressure, such as in the experiments reported by Fisher et al. [3]. More recently, whisker growths have been observed to form on another metal, aluminium held at 125°C. These whiskers were found [17] to grow to lengths of up to 200 μm from compressed thin-film aluminium deposits on silicon semiconductors. Such devices were found to fail as a result of leakage currents passing along whiskers that interconnected aluminium pads with adjacent gold bond wires. The author has also found that the electro-migration of aluminium along high-current-density paths will also create single-crystal whiskers and has demonstrated that these whiskers grow from grain boundary junctions, single grains, or hillocks [18]. These aluminium whiskers continued to grow until enough metal had been moved to equalise the local compressive stress on the conductor path.

Each of the pure metals that supports whisker growth from the base of the whisker is considered to be confined to the same growth mechanism. This would account for the remarkable similarity between the dimensions and surface morphologies of whiskers grown from either tin, cadmium, zinc or aluminium.

The exact cause and mechanism for the growth of tin whiskers has yet to be explained, although various documented theories do exist. Most of them are based on the theory of dislocation growth, and a fairly complete critical review of all of them has been given by Nabarro and Jackson [19].

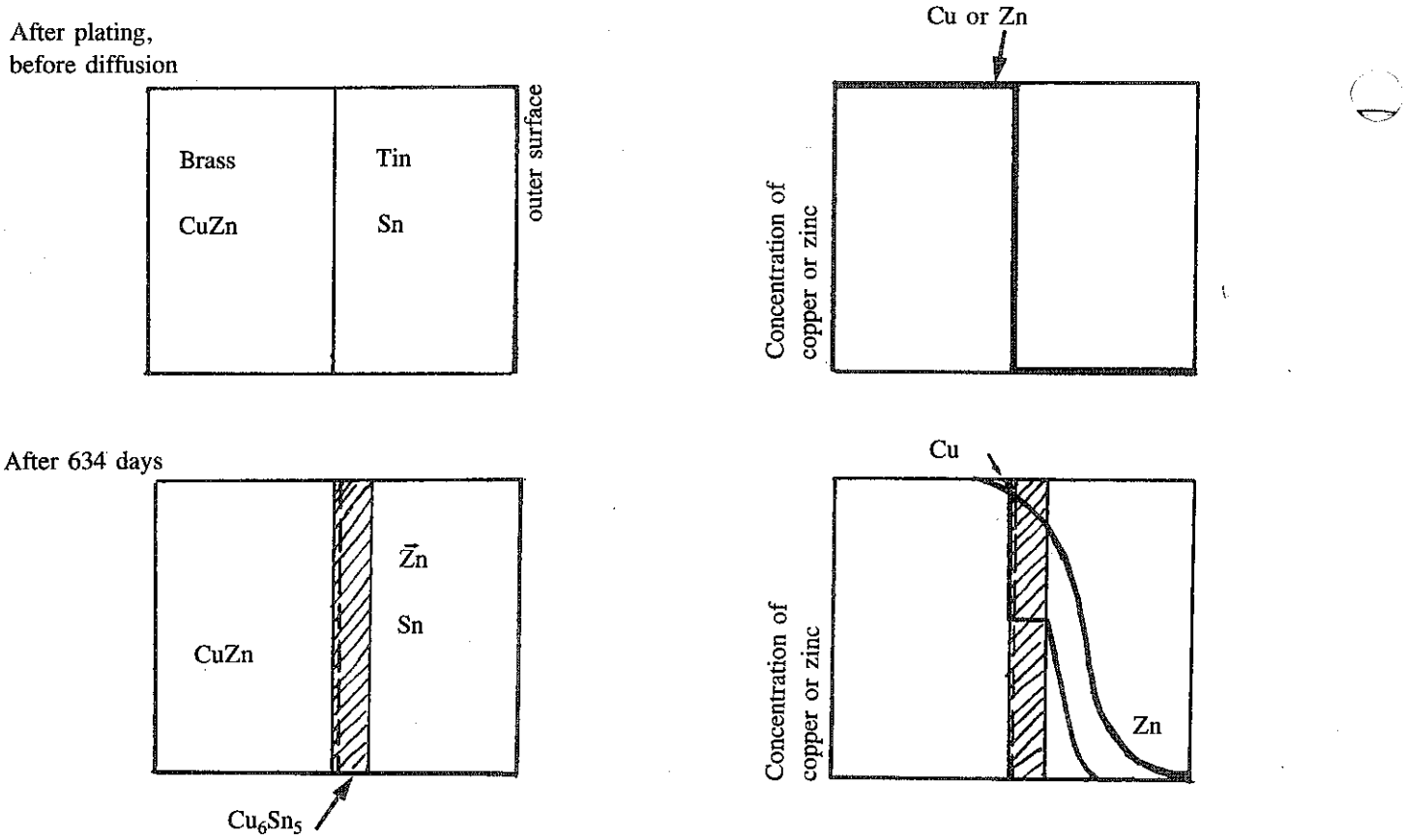

Figure 26. Interdiffusion of copper and zinc into tin after 634 d at room temperature (postulated).

One of the first theories was proposed by Frank [20]. An account is given starting with the assumption that whiskers form on dislocations. Frank regards the surface oxidation of the tin as the driving force for the extension of whiskers. This oxidation leads to stresses, particularly when a small knob of tin exists on a plated surface. With the aid of a screw dislocation, a continuous thread of metal is drawn from the main mass of tin. This dislocation/oxidation theory is contradicted by the findings of Arnold [1,21] and Carpenter [22] who have observed tin whiskers to grow under vacuum and when submerged in dielectric liquids, in each case in the absence of oxide films.

Several of the more likely theories have been reviewed in Reference 19 and condensed into one mechanism based on dislocation climb. The situation is considered in which a screw dislocation ends very near the surface of a crystal and is pinned there, for example by a foreign atom. To reach the surface, the dislocation must turn through a right angle, and then becomes an edge type. If the edge portion now turns around the anchoring point as a pole, it describes a spiral ramp, since after each turn the segment is displaced upwards by one lattice vector. Provided there is a suitable driving force, the whisker is then extruded. The whisker will rotate and grow in length as new atoms are placed onto, and turn, the screw dislocation.

The most recent, published, theory is the two-stage model for growth put forward by Lindborg [23]. He has proposed that zinc, tin and cadmium whisker growth consists initially of a climbing dislocation loop governed by the long-range diffusion of vacancies away from the loop in the bulk of the electroplate. When the loop reaches the plated surface, a whisker is formed by the presence of a one-atomic step in the direction of the Burger's vector. The second stage involves slip within the grains, and this is introduced by internal stresses. Material diffusion is controlled by the levels of internal stress causing slip and these levels will determine the rate, or acceleration, of whisker growth. Many of Lindborg's experiments were performed on different forms of zinc electroplate [24]. The prime driving force for whisker growth was stated to result from the internal macro-stresses built into the plating during electro-deposition. Also, the growth rate was dependent on the amount of macro-stresses present, slow or zero growth being observed for stresses below 4.5 kg/mm^2, a mixed region between 4.5 and 5.5 kg/mm^2 and a rapid growth region above 5.5 kg/mm^2. The maximum growth rates observed were 3 nm/s at 20°C. The driving force for whisker growth was not a result of micro-stresses or strain energy but, as previously stated, dependent on the presence of macro-stresses [24].

4.3 NEW PROPOSAL FOR NUCLEATION AND GROWTH

4.3.1 Background

We will turn our attention to the metallurgical findings of the tin-plated C-ring experiments. The preceding records and discussions of results do lend a limited support to the theories described in the previous paragraph. However, some of the driving forces are to be discounted and the order of stages for whisker growth proposed by Lindborg [23] have been modified.

4.3.2 The disputed effect of macro-stress

The major objection to previously published theories of whisker growth mechanism relates to the importance of *macro-stress*. Macro-stresses are considered here to include the stresses applied to tin plate by the mechanical deformation of its substrate material, direct loading of the tin plate by the application of a compression fastener, and the gross residual stresses that are long-range and result from internal macro-stress built into the tin plating during electro-deposition. The variations in macro-stress levels that were introduced by the author to the tin platings by deflection of the C-rings, were generally of the same order noted by other authors, including Frank [20] and Lindborg [23,24], to be necessary for macro-stess-induced whisker growth. Indeed, the 'highly' stressed C-rings (see Table 3) were designed to produce compressive stresses of up to 40 kg/mm^2, far in excess of those stresses previously shown to result in maximum rates of whisker growth by the 'squeeze' method [20]. The full results are recorded in Tables 4–8. 'Highly' stressed samples do not reflect short nucleation times for whisker growth, or support longer whiskers than observed on unstressed C-rings. Similarly, for any one sample, the surface areas of maximum stress (designated '*C*'), have no whisker-growth features that exceed those in the zero-stress areas, designated as '*A*', i.e. there is no

difference in the incidence or size of these whiskers. These observations are compounded by examination of Arnold's figures, presented in References 8 and 21. They show that the population density of whiskers grown in the compressive bend region of his samples was equal to that of growths occurring on flat, undisturbed areas as well as on plated areas external to the bend which would be under tensile stress.

It would also appear that macro-stress levels induced in the tin plated C-rings by abnormally high plating rates (see Table 1), which are generally considered to lock-in high stresses, also have no real effect on the whisker-growth rates. As a final observation, the areas of tin plating that surrounded the compression nut/washer (Fig. 2) have no real effect as preferential sites for whisker growth.

4.3.3 Micro-stress — the driving force for whisker growth

In view of the metallurgical results of this study, the dominant whisker-growth mechanism is considered to be dependent on the presence of *micro-stresses* within the tin platings. The energy for the growth of these whiskers is derived from relief of strain energy associated with the micro-stresses. Topographical observations, surface analyses and detailed metallography of the various samples have confirmed that metallurgical processes that include diffusion and recrystallisation do occur and may be expected to provide the driving forces for whisker growth.

The experimental results also confirm that whisker development is dependent on nucleation, growth and termination of growth. This sequence is remarkably similar to the events modelled in classical recrystallisation theory. Undoubtedly, there are additional factors to be taken into account, and these are included in the following paragraphs.

4.3.4 Solid-state diffusion, a source of micro-stresses

A discussion of whisker-growth mechanisms must include special reference to the series of growth photomicrographs taken after 57-, 181-, and 634-day inspection periods, which are presented in Figures 4–15. These show that high densities of large nodules exist on the tin-plated brass specimens. It would appear that, after plating, material is soon ejected from the tin-plate in the form of curly nodules having no preferential growth direction. Subsequently, either adjacent to or from within the nodule, the first whiskers are observed to grow. These whiskers usually have preferred growth directions, being remarkably cylindrical and either straight or with a small number of sharp kinks joining straight segments. At this stage, nodules are seen to be the precursors of whisker growth. Surface analyses show these nodules to be composed of tin with additions of zinc and traces of copper.

The shortest nucleation times for whisker growth occur on those samples having either brass substrates or an intermediate layer of copper plating. The high mobility of zinc within tin-plating has already been described. Copper also has a high diffusion mobility, but the results from other studies [25] prove that such diffusion anomalies in tin are not observed for solute atoms of iron. This lends support to the theory that the driving force for nucleation and growth of the initial tin whiskers is associated with the diffusion of zinc and copper. Hillert and Purdy [26] have shown that the diffusion of zinc along the grain boundaries of iron is accompanied by a surface relief on the iron surface in the vicinity of those boundaries. This was shown to result from the buildup of zinc and the associated increase in internal stress at these highly localised sites. The presence of zinc was also noted to induce grain-boundary migration. By a similar diffusion mechanism, zinc is also believed to have produced micro-stresses in the tin-plated brass C-rings. The logarithmic plots of maximum growth against time are shown in Figures 19–21. It would appear that the positive effect of zinc on the diffusion (both interstitial and grain-boundary) mechanism exceeds that of copper.

4.3.5 Intermetallic growth as a source of micro-stress

Recent studies by Fujiwara [27] using Auger depth profiling and X-ray diffraction have shown (by direct experimental evidence) that just 6 days after the deposition of electro-plated tin onto copper, a reaction resulted in the formation of the intermediate compound, Cu_6Sn_5. The existence of this layer was common to tin plate having different brightener additions and did not depend on the plating thickness of between 1 and 10 μm. This boundary layer of Cu_6Sn_5 was estimated [27] to have doubled in thickness between

room temperature storage periods of 6 days and 9 months. Fujiwara's findings confirm the intermetallic thicknesses observed in Figures 16 and 18 for the various stored samples of tin-plated brass and tin-plated copper. Thus, it seems that the solid-phase reaction at the tin/coppper interface proceeds quickly in its early stage. This is consistent with the fact, described previously, that the diffusion of copper into tin is rapid. The photomicrographs illustrate the fact that the growth front of Cu_6Sn_5 into the tin plate is more uniform when the substrate is composed of pure copper than the blocky, irregular front grown when the substrate is a copper/zinc alloy. The existence of intermetallic layers beneath tin and tin-lead platings is extremely important and it is considered to regulate both solderability and the rate of whisker growth. When reference is made to the densities of the various materials associated with tin-whisker growth, as presented in Table 12, it is clear that the formation of an intermetallic reaction layer will introduce micro-strains into the electroplate. The low-density tin-plate will be progressively replaced by a layer of Cu_6Sn_5 of higher density (and lower specific volume). The overall result of the intermetallic growth will be to compress the remaining tin layer and apply tension to the copper or brass substrate.

TABLE 12. *Room-temperature specific gravity of metals and intermetallics*

MATERIAL	DENSITY AT 20°C (g/cm^3)
Copper	8.96
Brass (60—40)	8.40
Steel (low C)	7.85
Zinc	7.14
Tin	7.30
Cu_3Sn	7.99
Cu_6Sn_5	8.26

* From private communication with Mr. J. Butler, Tin Research Institute, 1985

4.3.6 Low micro-stresses resulting in retarded whisker growth

Tin platings that exist on steel C-rings having no intermediate layer of copper will not be expected to undergo any solid-state diffusion mechanisms. Neither the iron nor the carbon from the steel are known to diffuse into tin. Also, reactions between iron and tin will only occur at temperatures approaching the melting point of tin [28]. The results for the steel substrates (Table 6) do not entirely confirm the hypothesis that no diffusion mechanisms exist, since evidence of whisker nucleation is seen on three of the nine specimens (i.e. 21−23) following extensive storage periods.

A review of the tabulated data collated for the organically contaminated tin platings indicates that the presence of such particles within the microstructure must somehow retard the diffusion process and, in turn, suppress the room-temperature stages of whisker nucleation and growth. Possibly, organic particles tend to block the drift of the vacancies that are necessary for basic diffusion to occur.

4.3.7 Secondary (pyramidal) tin whiskers

After a relatively long nucleation period, a new form of whiskers is seen to grow. These secondary whiskers (e.g. Figs. 4c,d) are pyramid-shaped with an increase in the number of longitudinal striations away from the growth direction. It is noticed that such stubby forms grow on copper and brass substrates and are the only whiskers to nucleate on the tin-plated steel samples (e.g. Fig. 11). These secondary whisker growths are not preceded at the same site by either nodules or cylindrical whiskers. The morphology of these secondary whiskers is very similar to that known to result from the thermal cycling of tin-plated printed-circuit boards [29]. Their growth is considered to result from the presence of micro-stresses introduced by the lateral expansion of second phases at the tin-to-substrate interface. In the case of the steel C-rings, these might be associated with the formation of rust spots.

4.3.8 Frank-Read sources and whisker growth by dislocation-climb

A surprising feature of the scanning electron micrographs and the optical photomicrographs is the fact that no depressions or other evidence of thinning of the electroplated finish has been observed, either:

- around the attachment point of large nodules
- around the base of exceedingly long whiskers, or
- in the case where many whiskers were growing in close proximity.

The above-mentioned observations again indicate that the basic growth mechanism for nodules and whiskers is diffusion related.

Examination of Figures 17 and 18 reveals that whisker growth occurs at a point below the tin-plated surface. It is indicated that rows of tin atoms are continually being forced up from the whisker growth site. The source could be a form of Frank-Read source and the mechanism for growth either one or a collection of interrelated screw dislocations. As whisker growth proceeds to release metal atoms, a corresponding volume of vacancies must form in the region beneath the whisker. Close examination of the whisker bases revealed no pits or holes that might have grown from vacancy clusters. Diffusion therefore apparently takes place through the plating over long radial distances from the whisker base.

4.3.9 The importance of grain boundaries

Grain boundaries are expected to account for the flux of tin atoms towards the Frank-Read source (they could also act as a sink for the vacancies). Such boundaries will tend to migrate when there is a difference in free energy per unit volume between adjoining tin grains. There will be a pressure on the boundary between them to move away from the lower-energy grain into the higher-energy one; this is called *'recrystallisation'* and has been accounted for in Section 4.1. The driving forces were seen to include increased strain in the plating (possibly resulting from the generation of Cn_6Sn_5 together with zinc and copper diffusion) and the presence of a high dislocation content that exceeds the stored energy of an adjacent grain.

4.3.10 The progressive influence of different driving forces in activating whisker growth

The crystallographic results show that no one crystallographic direction can be assigned to the long axis or growth direction. A feature of these results is that the observed directions favour low indices which are known to be slip directions in tetragonal tin and this is expected to be significant in understanding the growth process. The unusual crystal structures frequently observed on whisker growths are thought to reflect definite periodic changes in the growth mechanism (see, for instance, Fig. 13). The detailed whisker has nucleated as a very thin perfect single crystal, and the growth zone abruptly widens to increase the crystal's diameter. The kinked region appears to be attributable to a grain boundary or the growing together of several whiskers — certainly the parallelism of the segments shown in Figure 13 would not be fortuitous. One indication that dual growth is possible stems from the crystallographic results from whisker sample 5 (i.e. two single crystals were identified in Paragraph 3.5.1).

4.3.11 Possibility of Kirkendall voiding

A final observation refers to the cohesion properties of whisker-supporting tin-platings that have copper intermediate plating. In a previous evaluation it was noted that very low peel forces were required to separate these plated layers [30]. It has already been assumed that the process of whisker growth involves a diffusion mechanism. It would seem plausible that the occurrence of copper and/or zinc atoms migrating towards the tin surface by a vacancy diffusion mechanism may be associated with a form of the Kirkendall effect. It is postulated that, as diffusion progresses, bulges and compressive layers are present in the tin subsurface which will be conducive to whisker nucleation and growth. Simultaneously, vacancies migrate towards the tin/substrate interface to form pores or vacancy agglomerations that cause the markedly reduced cohesion that was observed experimentally.

4.4 SUMMARISED MODEL FOR WHISKER FORMATION

A comprehensive sequence of stages for the nucleation and growth of tin whiskers is proposed. There is a degree of agreement with the common requirements for growth published in the literature, namely:

(i) A dislocation must meet the surface.
(ii) A whisker emerges from the surface.
(iii) A driving force must exist to enable this transport mechanism to work.

The following stages, in which novel theories to account for more than one driving force have been proposed, summarise the events presented in Section 4.3.

Stage 1

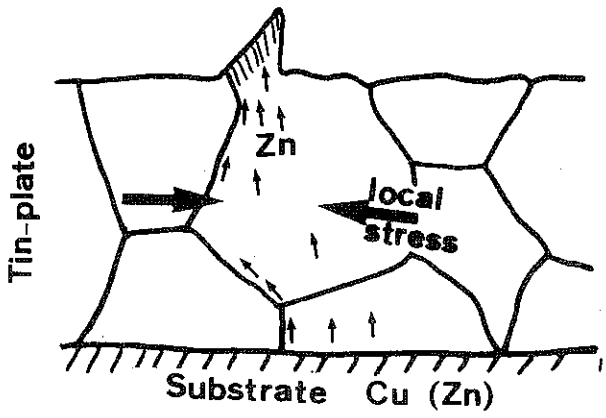

Nodular eruptions possessing no preferred crystallographic texture are pressed from individual grains of tin by localised micro-stress variations in neighbouring grains. This process will be enhanced by the diffusion of solute atoms (in particular zinc) giving rise to vacancy glide.

Stage 2

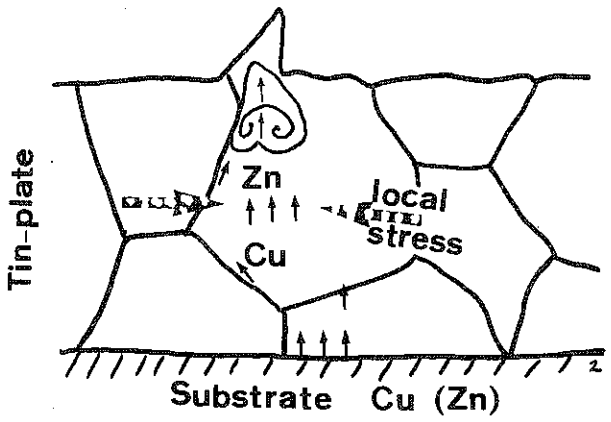

Once the large local stresses have been removed, diffusion continues to cause a stressed region adjacent to the surface. Frank-Read sources having suitable orientations may generate edge dislocations. Also, dislocations may be available from high-energy grain boundaries.

Whiskers are nucleated at preferential sites where the local degree of deformation is highest.

Stage 3

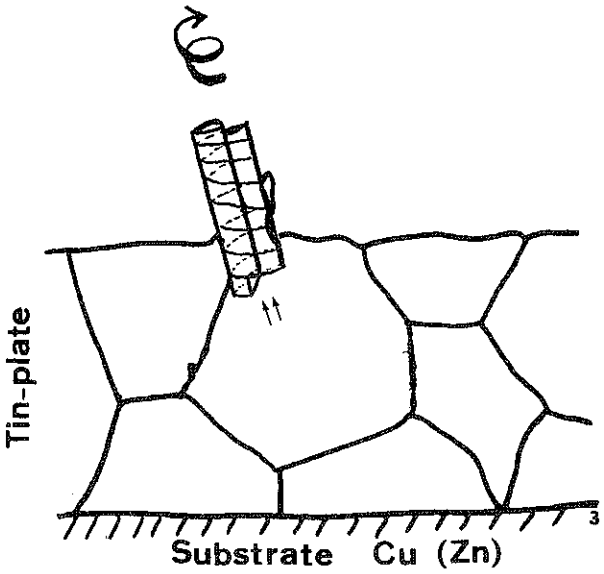

The edge dislocation is rotated to a screw segment. Atoms flow from the Frank-Read source or the grain boundary and attach themselves to the edge dislocation. This causes the screw segment to rotate and become displaced outwards (Fig. 8).

The treatment given to electrodeposition (Section 4.1) presupposes the existence of emerging screw dislocations onto which tin ions may be discharged. It is postulated that, should they become activated, such residual screw dislocations in the plating would be favourably oriented to sustain whisker growth.

Stage 4

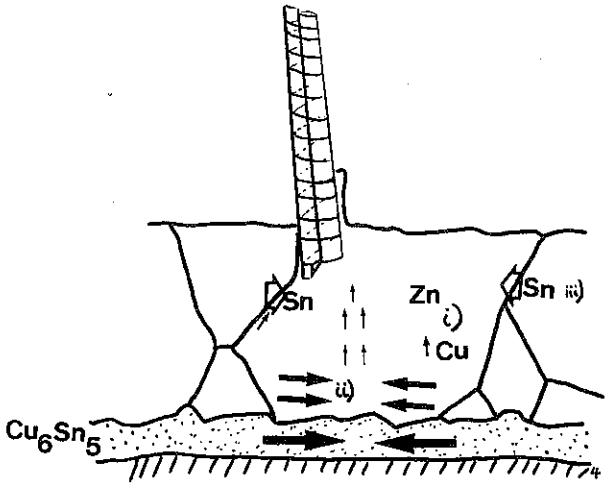

Growth of the whisker continues at a rate dependent upon the stresses generated in the grains (or grain

boundaries), resulting from one or more of the following diffusion-related mechanisms:

(i) diffusion of zinc and/or copper through tin (vacancies travel in reverse direction)
(ii) compressive pressure from intermetallic growth front
(iii) lateral diffusion of atoms by grain-boundary diffusion during recrystallisation (grain boundaries may be mobile).

Stage 5

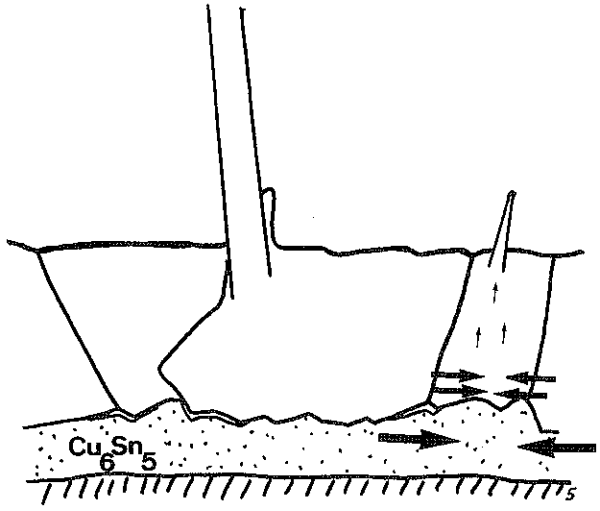

The process of recrystallisation will cease once the grain diameter has grown to a dimension approaching that of the plating thickness. Grain boundaries will be pinned by irregularities in the intermediate growth front and the *growth of primary whiskers will lose momentum.* Anisotropic growth of the intermetallic beneath grains having a preferred orientation may produce a secondary growth of whiskers once compressive forces in that grain reach a critical strain.

If there is no solute atom diffusion or intermetallic growth, the nucleation and growth of whiskers will depend only on the lateral diffusion of atoms at grain boundaries (i.e. Stage 4). This may explain the long incubation times for whisker growths on steel substrates. Alternatively, the driving force for these whiskers could result from the formation of iron oxide at the plating interface (oxygen can permeate through thin layers of as-plated tin).

4.5 METHODS FOR THE PREVENTION OF TIN-WHISKER GROWTH

A review of the reports published in the literature over the last 30 years provides conflicting information as regards advice on the most suitable precautions for the prevention of tin-whisker growths. Some of the discrepancies are likely to result from small differences in the tin-plating procedures used for finishing experimental samples or production hardware.

Of major importance is the variable nature of the whisker-growth nucleation period, which seems to vary enormously from one researcher's data to another's. The lack of growth after two years may cause the observer to record immunity to whisker growth, but in fact some whiskers have been reported to nucleate after storage periods of 8–10 years. Some whiskers in the present study were seen to nucleate after 3–5 years. The most frequently quoted work concerning the prevention of whisker growth is that of Britton [5]. He has listed a table of recommendations for reducing the risk of growths, which includes the following points (*the present author's comments appear in parenthesis*):

(a) Plating bath should be operated within the recommended process limits. (*Tables 4–8 show this to be ineffective; several C-ring types support more growths when a well-known commercial plating procedure is followed exactly; 'abnormal' procedures produces fewer whisker growths.*).

(b) Tin-plating on brass should be applied over an undercoat of nickel or copper. (*Possibly the nickel will increase whisker nucleation times, but the author's experiments show prolific growths when copper intermediate layers are employed.*)

(c) Coating thicknesses of electrodeposits not flow-melted should be at least 8 μm thick. (*Reference to Table 2 shows that 8 μm-thick deposits also show extensive growth. Also, a previous investigation found that deposits of 18–20 μm supported no whisker growths, whereas the same plating type, when only 10 μm thick, was strongly whisker-forming* [30].)

(d) Hot-dipped or flow-melted tin coatings are at far less risk than unheated electrodeposits. (*Supported by C-ring results, although the*

photomicrograph shown in Figure 10 indicates that nodular growth commences after 634 days of storage and Figure 15 clearly shows the formation of short whiskers after 1269 days.)

It is the author's opinion that no pure-tin-plating treatment will guarantee immunity from whisker growth for ever, particularly when such plated parts are subjected to an environment that may introduce micro-stresses into the plated layer and will include thermal cycling, static charging and particle irradiation. Tin plating, even when fused, should not be used in any high-reliability applications such as spacecraft construction. There are many alternative metal finishes that are not prone to whisker growths (such as silver, gold, tin-lead alloy etc.) and these have properties that are sufficiently similar to those of tin plating.

Probably the most suitable alternative finish to tin plating is the slightly hyper-eutectic composition of solder (63−65% tin, remainder lead). This solder alloy can be electroplated and then fused onto most metallic substrates [4]. Such a finish is identified as a mandatory ESA requirement for printed-circuit boards and terminations intended to support solder-mounted components [31]. A solder coating is also preferable to a tin coating for retention of solderability during long-term storage [9].

5. CONCLUSIONS

The results of a novel, comprehensive tin-whisker growth programme have been presented. They supplement data already published in the literature. A major finding was that compressive stresses applied to tin plate did not accelerate whisker growth rates. Incubation periods prior to whisker growth are shown to be strongly dependent on the substrate material. Tin-plated brass has a short (several days) nucleation period and produces whiskers with growth rates of 8 μm per day, whereas tin-plated steel takes several months to exhibit short whiskers. Nodular eruptions are frequently observed to precede those whiskers having a short incubation period. Most whiskers have parallel sides, but they may contain sharp kinks and can vary in diameter from around 6 μm down to only 6 nm. Straight whiskers approaching 2 mm in length have been observed. They were noted to change their orientation during growth, and by rotating became ensnarled with other growths. Their population density can reach 300 per mm^2. Metallography revealed that, despite the relatively large volume of tin material being ejected in the form of nodules and long whiskers, there was no evidence of depressions or local subsidences in the plated layer. Crystallography has identified five tin-whisker growth directions and with TEM work has shown the whiskers to be single crystals containing no dislocations or second phases. Attempts to promote the white-to-grey tin allotropic transformation at cryogenic temperatures were unsuccessful.

A five-stage model for whisker growth has been proposed, based on the premise that local micro-stresses can be eliminated by the ejection of tin atoms from the plated layer at sites of rotating screw dislocations. It is also postulated that a long-range atom-transport mechanism (diffusion) sustains these growths.

It is strongly recommended that surfaces known to support whisker growth be excluded from all high-reliability applications — plated layers of tin, cadmium and zinc can be replaced by an electroplated, then fused, tin/lead alloy. One sample of fused tin platings has initiated whisker growth after a storage period of 3–5 years and longer incubation periods for the remaining samples having this finish cannot yet be ruled out.

REFERENCES

1. Arnold, S.M., Growth and properties of metal whiskers. *Proc. 43rd Am. Electroplaters Soc.*, 26 (1956).
2. Britton, S.C., Spontaneous growth of whiskers on tin coating. *Trans. Inst. of Metal Finishing*, **52**, 95 (1974).
3. Fisher, R.M., Darken, L.S. & Carroll, K., Accelerated growth in tin whiskers. *Acta Met.* **2**, 368 (1954).
4. Dunn, B.D., The fusing of tin-lead plating on high-quality printed-circuit boards. *Trans. Inst. Metal Finishing*, **58**, 26 (1980).
5. Fernandez, S.O. & Tisinai, G.F., Stress analysis of unnotched C-rings. *J. Eng. for Industry*, Feb., 147 (1968).
6. Timoshenko, S., *Strength of Materials.* Part 1, Chapter XII, Third Edn., Van Nostrand.
7. Price, J.W., *Tin and tin-alloy plating.* Electromechanical Publications Ltd., Ayr (1983).
8. Ellis, W.C., Gibbons, D.F. & Treuting, R.G., Growth of metallic whiskers from the solid. *Growth and perfection of crystals.* John Wiley & Sons, New York. 102 (1958).
9. Brandes, E.A., Smithells Metals Reference Book, Chapter 4. Butterworth and Co. (1983).
10. Burgers, W.G. & Groen, L.J., Mechanism and kinetics of the allotropic transformation of tin. Discussions Faraday Soc. **23**, 183 (1957).
11. Gabe, D.R., *Principles of Metal Surface Treatment and Protection.* 2nd Edition. Pergamon Press, Oxford (1978).
12. Cahn, R.W., *Physical Metallurgy.* 2nd Edition. North-Holland Pub. Co., Amsterdam (1970).
13. Barrett, C.S., *Structure of Metals.* McGraw Hill Book Co., New York (1952).
14. Guy, A.G., *Elements of Physical Metallurgy.* 2nd Edition. Addison–Wesley Pub. Co. (1970).
15. Dunn, B.D., Produktsicherung bei der Auswahl von Material und Verbindingen für Satelliten. *Metall*, **8**, 711 (1976).
16. Bouquet, G., Dubois, B. & Langeron, J.P., Recristallisation, après déformation, de monocristaux d'étain blanc. *Mémoires Scientifiques de la Revue de Metallurgies (Paris)*, **66**(10), 731 (1969).
17. Turner, T.E. & Parsons, R.D., A new failure mechanism: Al-Si bond pad whisker growth. *IEEE Trans.*, **CHMT-5**(Dec.), 431 (1982).
18. Dunn, B.D., to be published.
19. Nabarro, F.R. & Jackson, P.J., Growth of crystal whiskers. *Growth and Perfection of Crystals*, John Wiley and Sons, New York. 11 (1958).
20. Frank, F.C., On tin whiskers. *Phil. Mag.*, **44**, 854 (1953).
21. Arnold, S.M., Growth of metal whiskers on electrical components. *Proc. Electrical Components Conference*, 75 (1959).
22. Carpenter, C.L., Lockheed Restricted Note.
23. Lindborg, U., A model for the spontaneous growth of zinc, cadmium and tin Whiskers. *Acta Met.* **24**, 181 (1976).
24. Lindborg, U., Observations on the growth of whisker crystals from zinc electroplate. *Met. Trans. A*, **16**(August), 1581 (1975).
25. Brik, V.B., Regular features of the diffusion motion of iron and cobalt atoms in high purity tin. *Phys. Met. Metall.* **53**, 176 (1982).
26. Hillert, M. & Purdy, G.R., Chemically induced grain boundary migration. *Acta Met.* **26**, 333 (1978).
27. Fujiwara, K. et al., Interfacial reaction in bimetallic Sn/Cu thin films. *Thin Solid Films*, **70**, 153 (1980).
28. Philofsky, E., Intermetallic formation on gold-aluminium systems. *Solid-State Electronics*, **13**, 1391 (1970).
29. Dunn, B.D., to be published.
30. Dunn, B.D., Whisker formation on electronic materials. *ESA Sci. Tech. Rev.* **2**, 1 (1976).
31. Product Assurance Division, ESTEC, *The qualification and procurement of two-sided printed-circuit boards (fused tin-lead or gold-plated finish).* ESA PSS-01-710 Issue 1, October 1985.